

---

**Research Articles: Behavioral/Cognitive**

**The neural basis of aversive Pavlovian guidance during planning**

Níall Lally<sup>1,2</sup>, Quentin J M Huys<sup>3,4</sup>, Neir Eshel<sup>5</sup>, Paul Faulkner<sup>6,1</sup>, Peter Dayan<sup>7</sup> and Jonathan P Roiser<sup>1</sup>

<sup>1</sup>*Institute of Cognitive Neuroscience, University College London, Alexandra House, 17 Queen Square, London, WC1N 3AR, UK.*

<sup>2</sup>*Experimental Therapeutics and Pathophysiology Branch, NIMH, NIH, Bethesda, MD, USA.*

<sup>3</sup>*Translational Neuromodeling Unit, Institute of Biomedical Engineering, University of Zurich and ETH Zurich, Switzerland.*

<sup>4</sup>*Centre for Addictive Disorders, Department of Psychiatry, Psychotherapy and Psychosomatics, Hospital of Psychiatry, University of Zurich, Switzerland.*

<sup>5</sup>*Department of Psychiatry and Behavioral Sciences, Stanford University School of Medicine, CA, USA.*

<sup>6</sup>*Semel Institute for Neuroscience and Human Behaviour, University California, Los Angeles.*

<sup>7</sup>*Gatsby Computational Neuroscience Unit, University College London, 25 Howland Street, London, W1T 4JG, UK.*

DOI: 10.1523/JNEUROSCI.0085-17.2017

Received: 11 January 2017

Revised: 19 June 2017

Accepted: 18 July 2017

Published: 18 September 2017

---

**Author Contributions:** Conceptualization, J.P.R., N.L., N.E., P.D., and Q.J.M.H.; Design, J.P.R., N.L., N.E., P.D., and Q.J.M.H.; Data collection, N.L., and P.F.; Writing -- Original Draft, J.P.R., N.L., N.E., P.D., P.F., and Q.J.M.H.; Writing -- Review & Editing J.P.R., N.L., N.E., P.D., P.F., and Q.J.M.H.; Funding Acquisition, J.P.R. and P.D.; Resources, J.P.R.; Supervision, J.P.R.

**Conflict of Interest:** The authors declare no competing financial interests.

We thank Nathaniel Daw for discussions and comments on an earlier draft of the manuscript.

This work was funded by a British Academy grant (BR10030) to JPR. NL was funded by a Wellcome Trust-National Institutes of Health joint PhD studentship (WT095465). PF was funded by an MRC studentship. PD is funded by the Gatsby Charitable Foundation. The funders had no role in the study design, data collection and interpretation, or the decision to submit the work for publication.

**Correspondence:** [niall.lally@gmail.com](mailto:niall.lally@gmail.com) (N. L.), [qhuys@cantab.net](mailto:qhuys@cantab.net) (Q. J. M. H.)

**Cite as:** J. Neurosci ; 10.1523/JNEUROSCI.0085-17.2017

**Alerts:** Sign up at [www.jneurosci.org/cgi/alerts](http://www.jneurosci.org/cgi/alerts) to receive customized email alerts when the fully formatted version of this article is published.

Accepted manuscripts are peer-reviewed but have not been through the copyediting, formatting, or proofreading process.

Copyright © 2017 the authors

1

Pages: 33

2

Figures: 5

3

Tables: 2

4

## 5 **The neural basis of aversive Pavlovian guidance during planning**

6

7 Níall Lally<sup>1,2,8</sup>✉, Quentin J M Huys<sup>3,4,8</sup>✉, Neir Eshel<sup>5</sup>, Paul Faulkner<sup>6,1</sup>, Peter Dayan<sup>7</sup>, and  
8 Jonathan P Roiser<sup>1</sup>

9 <sup>1</sup>Institute of Cognitive Neuroscience, University College London, Alexandra House, 17 Queen  
10 Square, London, WC1N 3AR, UK.

11 <sup>2</sup>Experimental Therapeutics and Pathophysiology Branch, NIMH, NIH, Bethesda, MD, USA.

12 <sup>3</sup>Translational Neuromodeling Unit, Institute of Biomedical Engineering, University of Zurich  
13 and ETH Zurich, Switzerland.

14 <sup>4</sup>Centre for Addictive Disorders, Department of Psychiatry, Psychotherapy and  
15 Psychosomatics, Hospital of Psychiatry, University of Zurich, Switzerland.

16 <sup>5</sup>Department of Psychiatry and Behavioral Sciences, Stanford University School of Medicine,  
17 CA, USA.

18 <sup>6</sup>Semel Institute for Neuroscience and Human Behaviour, University California, Los Angeles.

19 <sup>7</sup>Gatsby Computational Neuroscience Unit, University College London, 25 Howland Street,  
20 London, W1T 4JG, UK.

21 <sup>8</sup>These authors contributed equally

22

23 For submission to *The Journal of Neuroscience* as a *research report*.

24

25 ✉: [niall.lally@gmail.com](mailto:niall.lally@gmail.com) (N. L.), [ghuys@cantab.net](mailto:ghuys@cantab.net) (Q. J. M. H.)

**26 Abstract**

27 Important real-world decisions are often arduous as they frequently involve sequences of  
28 choices, with initial selections affecting future options. Evaluating every possible  
29 combination of choices is computationally intractable, particularly for longer multi-step  
30 decisions. Therefore, humans frequently employ heuristics to reduce the complexity of  
31 decisions. We recently used a goal-directed planning task to demonstrate the profound  
32 behavioral influence and ubiquity of one such shortcut, namely aversive pruning, a reflexive  
33 Pavlovian process that involves neglecting parts of the decision space residing beyond  
34 salient negative outcomes. However, how the brain implements this important decision  
35 heuristic, and what underlies individual differences have hitherto remained unanswered.  
36 Therefore, we administered an adapted version of the same planning task to healthy male  
37 and female volunteers undergoing functional magnetic resonance imaging (fMRI) to  
38 determine the neural basis of aversive pruning. Through both computational and standard  
39 categorical fMRI analyses, we show that when planning was influenced by aversive pruning,  
40 the subgenual cingulate cortex was robustly recruited. This neural signature was distinct  
41 from those associated with general planning and valuation, two fundamental cognitive  
42 components elicited by our task but which are complementary to aversive pruning.  
43 Furthermore, we found that individual variation in levels of aversive pruning were  
44 associated with the responses of insula and dorsolateral prefrontal cortex to the receipt of  
45 large monetary losses, and also with sub-clinical levels of anxiety. In summary, our data  
46 reveal the neural signatures of an important reflexive Pavlovian processes that shapes goal-  
47 directed evaluations, and thereby determines the outcome of high-level sequential cognitive  
48 processes.

**49 Significance Statement**

50 Multi-step decisions are complex because initial choices constrain future options. Evaluating  
51 every path for long decision sequences is often impractical; thus, cognitive shortcuts are  
52 often essential. One pervasive and powerful heuristic is aversive pruning, in which potential  
53 decision-making avenues are curtailed at immediate negative outcomes. We used  
54 neuroimaging to examine how humans implement such pruning. We found it to be  
55 associated with activity in the subgenual cingulate cortex, with neural signatures that were  
56 distinguishable from those covarying with planning and valuation. Individual variations in  
57 aversive pruning levels related to sub-clinical anxiety levels and insular cortex activity. These  
58 findings reveal the neural mechanisms by which basic negative Pavlovian influences guide  
59 decision-making during planning, with implications for disrupted decision-making in  
60 psychiatric disorders.

61 **Introduction**

62 Most important decisions are difficult as they involve sequences of consequential  
63 choices. For example, to go to university, where, and what to study? Such planning is  
64 complex as the outcomes of earlier decisions (e.g. degree) can affect the availability  
65 of later options (e.g. income), and the resulting tree of future possibilities to be  
66 evaluated grows quickly with decision sequence length. To manage this intricacy, we  
67 often have to abandon rational calculation in favour of hard-wired approximations.  
68 We recently identified one such powerful Pavlovian heuristic that humans  
69 ubiquitously use during complex planning, which we term “aversive pruning” (Huys  
70 *et al.*, 2012). Aversive pruning entails excising from consideration decision tree  
71 branches that contain important negative events (here, large monetary losses;  
72 **Figures 1A-B**). Individual variation in aversive pruning levels predicted the severity of  
73 subclinical depressive symptoms (Huys *et al.*, 2012), suggesting a possible role in  
74 depression (Dayan and Huys, 2008, Eshel and Roiser, 2010). These behavioural and  
75 computational studies raise the question as to how aversive pruning is implemented  
76 in the brain. Therefore, we sought to identify the neural basis of aversive pruning  
77 using fMRI.

78 Aversive pruning is reflexive, akin to Pavlovian responses, as it persists above  
79 and beyond loss aversion, even when it is highly suboptimal (Huys *et al.*, 2012). Our  
80 central expectation therefore was that aversive pruning would be mediated via  
81 regions known to be involved in orchestrating emotional reactions to aversive  
82 events. Thus, our predictions focused first on the subgenual anterior cingulate cortex  
83 (SGC; part of the ventromedial prefrontal cortex). The SGC is anatomically well  
84 placed to subserve the impact of affective aversive values on planning. It is  
85 connected to areas involved in mediating Pavlovian behavioural inhibition such as  
86 the periaqueductal grey (PAG) and amygdala, as well as regions involved in the  
87 evaluation required for planning (Schultz, 2015), such as orbitofrontal cortex (OFC)  
88 and dorsolateral prefrontal cortex (DLPFC; (Johansen-Berg *et al.*, 2008, Ongur *et al.*,  
89 2003). The SGC is known to both represent aversive stimuli and mediate their  
90 impact: neurons in the homologous region of the macaque brain (ventral bank of the  
91 pregenual anterior cingulate) specifically represent negatively-valenced motivational  
92 value (Amemori and Graybiel, 2012). These neurons increased in activity during  
93 decisions to avoid a punishment (facial air puff), which also entailed forsaking a  
94 reward (food). Importantly, stimulation of these neurons triggered maladaptive  
95 decision-making, increasing levels of avoidance even when potential concomitant  
96 rewards were high.

97 There is also evidence that the SGC participates in aversive processing in  
98 humans (Talmi *et al.*, 2009). Additionally, and consistent with some theoretical  
99 accounts of the role that Pavlovian inhibition plays in the development of affective  
100 disorders (Dayan and Huys, 2008, Eshel and Roiser, 2010, Huys *et al.*, 2015a), the  
101 SGC has consistently been shown to be overactive in patients with mood disorders  
102 (Drevets *et al.*, 1997, Drevets *et al.*, 2008), with its degree of activation to negative  
103 stimuli predicting treatment response in depression (Roiser *et al.*, 2012). Since  
104 aversive pruning is a form of reflexive behavioural inhibition, we additionally  
105 expected the involvement of regions directly implicated in this process, notably the  
106 PAG and amygdala. The PAG participates in fear (Mobbs *et al.*, 2007) and increases

## Neural Basis of Aversive Pruning

107 in activation with anxiety in humans (Mobbs *et al.*, 2010). The amygdala has been  
108 reported to be recruited during human conditioned inhibition (Geurts *et al.*, 2013).  
109 Both structures have also been implicated in affective disorders (Krishnan and  
110 Nestler, 2008).

111 Finally, as planning depends on multiple cognitive systems, we anticipated  
112 that the neural architecture subserving aversive pruning would operate in addition  
113 to, yet distinct from, established networks governing other cognitive processes.  
114 Specifically, we expected to distinguish the neural correlates of aversive pruning  
115 from those associated with executive functioning (Newman *et al.*, 2003) and  
116 mnemonic processes (Tolman, 1948) (DLPFC, parietal cortex, dorsal striatum),  
117 sequence planning (Fermin *et al.*, 2016, Matsuzaka *et al.*, 2012) (pre-supplementary  
118 motor area (SMA), SMA, motor cortex, cerebellum), as well as goal-directed  
119 evaluation (Schultz, 2015) (ventral striatum, OFC, insula).

120 **Materials and methods**121 **Participants**

122 Forty-one healthy volunteers (21 female; M = 23.30 years, SD = 3.70) were recruited  
123 via the University College London Psychology participant pool. Participants were  
124 screened for past and present psychiatric disorders, including substance/alcohol  
125 dependence/abuse, using the Mini International Neuropsychiatric Inventory  
126 (Sheehan *et al.*, 1998). Past or present psychopathology was an exclusion criterion  
127 and one participant was excluded on this basis (previous substance dependence),  
128 leaving 40 participants in the analysis. Participants completed the State-Trait Anxiety  
129 Inventory (STAI; (Spielberger *et al.*, 1970); state: M = 9.50, SD = 7.20, trait: M =  
130 14.00, SD = 7.53), Beck Depression Inventory (BDI; (Beck *et al.*, 1961); M = 3.13, SD =  
131 4.21), the revised Neuroticism-Extraversion-Openness Personality Inventory (NEO PI-  
132 R; (Costa and McCrae, 1992); openness: M = 33.28, SD = 5.84, conscientiousness: M =  
133 29.90, SD = 7.88, extraversion: M = 31.45, SD = 6.54, agreeableness: M = 34.18, SD  
134 = 4.84, neuroticism: M = 17.98, SD = 8.13) and the Wechsler Test of Adult Reading  
135 (WTAR; (Wechsler, 2001)), which was used to evaluate intelligence quotient (IQ; M =  
136 111, SD = 4.2). The study was approved by the UCL Graduate School Ethics  
137 Committee and all participants provided written, informed consent. Participants  
138 were compensated based on task performance, up to a maximum of £40, with a  
139 minimum payment of £15.

140 **Figure 1 about here**

141 **Task**

142 The reinforced sequential planning task was adapted for fMRI from one described in  
143 detail previously (Huys *et al.*, 2012) and programmed in Cogent 2000  
144 ([www.vislab.ucl.ac.uk/Cogent](http://www.vislab.ucl.ac.uk/Cogent)), a stimulus presentation toolbox for Matlab (version  
145 7.1). Participants moved throughout a hexagonal maze via button presses (U/I during  
146 training, left/right in the scanner; **Figure 1C**) in an attempt to maximize earnings.  
147 Possible outcomes (**Figure 1D**) comprised one large reward (+140 pence, top blue  
148 arrow), three large losses (-70 pence, red arrows), and several small gains and losses  
149 (20 pence each, green (+) and black (-) transitions, respectively). During free plan  
150 trials (of which there were 90; **Figure 1E**), participants had nine seconds to devise a  
151 sequence of moves so as to maximize their earnings (planning phase); a countdown  
152 timer from 9 to 1 indicated the amount of time left in seconds. Following this  
153 planning phase, participants had 2.5 seconds to input their responses, via a series of  
154 button presses on an MRI-compatible button box. We biased the free plan trials by  
155 starting position and difficulty, such that for 60 trials it was optimal to transition  
156 through the large loss, while for the remaining 30, the optimal sequence avoided the  
157 large loss.

158 During restricted plan trials (40; **Figure 1F** and **1G**), participants were  
159 presented with two possible multi-step routes (equal length; 3-5 moves) through the  
160 maze, one coloured blue and the other green (**Figure 1F**), and had to choose  
161 between just these. As in the free plan trials, participants had nine seconds to  
162 evaluate the best route (one path always yielded more money than the other).  
163 Subsequently, two coloured boxes appeared, one blue, the other green, and the  
164 participant then selected their chosen route with a single button press (either left or

## Neural Basis of Aversive Pruning

165 right option, **Figure 1G**; again, as per free plan trials, participants had 2.5 seconds to  
166 input their response). Twenty of the restricted plan trials involved deciding between  
167 two routes that both transitioned through a large loss (restricted plan large loss). In  
168 the other 20 restricted plan trials, both paths avoided the large loss (restricted plan  
169 no large loss).

170 For both free plan and restricted plan trials, participants were then shown  
171 the selected sequence of moves and their corresponding monetary outcome (0.8 s  
172 for each move; **Figure 1H**). Every trial finished with a fixation cross, which varied in  
173 duration depending on the number of moves (0.5-2.1 s), such that the trial duration  
174 was always 16 seconds. Twenty fixation trials, also 16 seconds in duration, were  
175 included to constitute an implicit baseline in the fMRI analysis. Trials were  
176 randomized into three runs of 50 trials, each lasting 13.5 minutes and with the  
177 constraint that no trial (i.e. number of moves, starting position and trial type) was  
178 repeated consecutively. Participants were paid according to their earnings, but the  
179 running net income was not displayed until the end of each run. Not entering  
180 enough moves on free plan trials, or failing to respond on restricted plan trials,  
181 incurred a £2 loss on each occasion.

182 Participants received extensive training on the task before entering the  
183 scanner: 30 trials without reinforcement, followed by a test, to learn the transitions  
184 (**Figure 1C**); and 34 trials to learn the transition values (**Figure 1D**), including 18 free  
185 plan and two restricted plan trials with no time restriction, and 14 with the same  
186 time restriction as in the scanner, two of which were restricted plan trials.

187

## 188 Behavioural analyses

### 189 Basic behavioural outcome measures

190 Free plan trials were classified according to the following categories: correct  
191 decisions (participants executed the best possible sequence), suboptimal decisions  
192 (participants did not execute the best possible sequence), and misses (participants  
193 failed to enter enough moves). Correct decisions were further sub-categorised as  
194 “optimal large loss” (OLL) correct trials, on which the participant transitioned  
195 through at least one large loss to gain the maximum amount of money, and “optimal  
196 no large loss” (ONLL) correct trials, where the maximum was attained by avoiding  
197 large losses. Suboptimal decisions were further classified into “aversive pruning”  
198 trials and “error” trials. Aversive pruning trials were defined when it was optimal to  
199 transition through the large loss, but participants selected the best available option  
200 that avoided the large loss (e.g. **Figure 1A-B**). Errors were defined as all other  
201 instances of suboptimal choices and were subdivided into trials where the optimal  
202 decision would avoid (ONLL error, though these occurred very rarely) or entail (OLL  
203 error, excluding aversive pruning trials) transitioning through a large loss. Restricted  
204 plan trials were classified as either correct or errors. Please see **Table 1** for a list of  
205 trial outcome classifications.

206 The main behavioural outcome measures were proportion correct (OLL and  
207 ONLL) scores (after removing the small number of missed trials: mean = 4.65%, SD =  
208 2.55%) and reaction times (calculated at the time of the first move entered). We



## Neural Basis of Aversive Pruning

209 determined a proxy (trial-based) measure of each individual's sensitivity to large  
 210 losses by calculating the difference between ONLL and OLL correct scores (averaged  
 211 across depth). We excluded three participants who scored below 50% correct across  
 212 all ONLL trials, indicating an inability to perform the task.

213 **Table 1.** Basic behavioural outcome measures

Type	Abbreviation	Explanation
Optimal no large loss correct	ONLL correct	Optimal sequence chosen where this does not include a large loss
Optimal large loss correct	OLL correct	Optimal sequence chosen where this includes a large loss
Aversive pruning	-	The best sequence that avoids large losses chosen when the optimal sequence includes at least one
Optimal no large loss error	ONLL error	Suboptimal sequence chosen for this trial type, not including aversive pruning
Optimal large loss error	OLL error	All suboptimal sequences chosen for this trial type

214

215 **Basic behavioural data analyses**

216 Behavioural data from the scan (i.e. excluding training trials) were analysed using  
 217 SPSS (Software Package for Statistics and Simulation; Version 21. NY, USA: IBM  
 218 Corp). Only free and restricted plan trials on which participants entered the correct  
 219 number of moves were included in this analysis. Accuracy, reaction time (RT) and  
 220 earnings data across conditions were analysed using paired-sample *t*-tests and  
 221 analysis of variance (ANOVA). Due to low trial numbers, RT and earnings data were  
 222 not analysed for ONLL error trials. Where appropriate, RT data were log transformed  
 223 to meet parametric assumptions (assessed using the one-sample Kolmogorov-  
 224 Smirnov test). Where transformations were not sufficient to correct normality  
 225 violations, non-parametric tests were applied, including the Friedman test and  
 226 Wilcoxon Signed-rank test. To test the relationship between psychometric variables  
 227 and task performance, we used multiple linear regression, with the following  
 228 variables included in the model: age, sex, IQ, STAI trait, STAI state and BDI. For all  
 229 analyses,  $P < 0.05$  was considered significant and  $0.05 < P < 0.1$  a trend towards  
 230 significance. Where appropriate, Greenhouse-Geisser correction of degrees of  
 231 freedom was used to accommodate violations of sphericity.

232

233 **Model-based behavioural data analyses**

234 *Overview of model-based behavioural data analyses*

235 Here, we focussed our analyses specifically on aversive pruning and fMRI; detailed  
 236 analyses of alternate planning strategies are described elsewhere (Huys *et al.*,  
 237 2015b). Computational modelling was based on our previous approach (Huys *et al.*,  
 238 2012). Only free plan trials on which participants entered sufficient moves were  
 239 included; restricted plan trials were not modelled. Following model fitting, models  
 240 were compared using the integrated Bayesian information criteria (iBIC; (Huys *et al.*,



241 2012), in which models of greater complexity are penalized more strongly, and thus  
 242 are required to have higher log likelihoods for the choices than simpler models.

243 We initially provide a brief overview of our modelling approach, and explain  
 244 this in more detail in the section below. Our analyses focussed on the creation of  
 245 four distinct computational models and their evaluation in relation to our  
 246 behavioural data based on our previous results with this task reported in Huys et al.,  
 247 (2012). First, we constructed an optimally performing model, called “Lookahead”,  
 248 which fully evaluated each sequence within the maze and chose the path with the  
 249 highest net total value. As optimal sequence planning is unrealistic, especially at  
 250 higher decision depths, we next calculated a “Discount” model, in which sequence  
 251 planning is probabilistically terminated at each depth, with the likelihood of  
 252 termination determined by the “general discount” parameter. Most relevant to the  
 253 hypothesis examined here, we then created a “Pruning” model, in which participants  
 254 stopped planning sequences specifically if they contained a large monetary loss, in  
 255 addition to general discounting. This tendency is governed by the “pruning” (specific  
 256 discount) parameter. Finally, we constructed a “Loss sensitive” model to control for  
 257 any overweighting of negative relative to positive outcomes, a phenomenon  
 258 commonly known as loss aversion.

259 For the fMRI analyses, we exploited the best-fitting, Pruning model, to  
 260 quantify the “inclination to prune” on a trial-by-trial basis. This involved computing  
 261 the distribution of probabilities over all possible paths for a particular problem  
 262 (starting state and depth), given that individual’s pruning parameter. This  
 263 distribution was calculated from the “Pruning” model. We also computed this  
 264 distribution assuming that the pruning parameter was identical to the general  
 265 discount parameter – in other words, assuming no specific discounting when  
 266 encountering large monetary losses, equivalent to the “Discount” model. The  
 267 difference between these two distributions, calculated for every trial, was our metric  
 268 of the inclination to prune in our model-based fMRI analyses, and is called the  
 269 Kullback-Leibler (KL) divergence.

270 *Details of model-based behavioural data analyses*

271 Compared with our previous approach (Huys *et al.*, 2012), the models were adapted  
 272 to take into account the fact that participants had to emit an entire action sequence  
 273 at once; the models therefore had to specify distributions over entire action  
 274 sequences. That is, rather than choosing from one of the two actions  $d$  times (as  
 275 previously (Huys *et al.*, 2012),  $D$  corresponds to decision depth), participants chose  
 276 one sequence from the entire set of  $2^D$  available sequences. We write the probability  
 277 of emitting sequence  $\mathbf{a}^i$  as:

$$278 \quad p(\mathbf{a}^i) = \frac{\exp(\beta Q(\mathbf{a}^i))}{\sum_j \exp(\beta Q(\mathbf{a}^j))} \quad [1]$$

279 where  $\beta$  is the inverse temperature which determines the steepness of the softmax  
 280 function.

281 The  $Q$  value was defined as follows. For model “Lookahead”, a standard tree-  
 282 search algorithm was used. This completely evaluates each possible sequence  
 283 according to the sum of all  $D$  outcomes  $r_d(\mathbf{a}^i)$  that would be encountered:

## Neural Basis of Aversive Pruning

$$Q^{\text{look}}(\mathbf{a}^i) = \sum_{d=1}^D r_d(\mathbf{a}^i) \quad [2]$$

285 However, it is computationally unrealistic for human participants to perform  
 286 such a search, given the large number of possible sequences (8, 16 or 32 sequences,  
 287 for 3-, 4- and 5-move trials respectively). Thus, we fitted a “Discount” model, which  
 288 captures the tendency not to plan fully, forcing the tree search to terminate at each  
 289 depth with probability  $1-\gamma$  (hence  $\gamma$  here represents the continuing probability; note  
 290 that in Huys *et al.* 2012 it was formulated as the complementary stopping  
 291 probability). The ‘Discount’ model captured such uniform search curtailment with a  
 292 single  $\gamma$  parameter:

$$Q^{\text{disc}}(\mathbf{a}^i) = \sum_{d=1}^D \gamma^{d-1} r_d(\mathbf{a}^i) \quad [3]$$

294 The next model, “Pruning” is central to the hypothesis we aimed to test here:  
 295 it splits the  $\gamma$  parameter into  $\gamma_G$  (“general pruning”) representing the general  
 296 tendency not to plan (as in model discount), and  $\gamma_S$  (termed “specific pruning” in our  
 297 previous report (Huys *et al.*, 2012); here “aversive pruning”) the probability of tree-  
 298 search continuation specifically on encountering a large loss. The “Pruning” model  
 299 incorporated these two separate  $\gamma$  parameters:

$$Q^{\text{prune}}(\mathbf{a}^i) = \sum_{d=1}^D \gamma_G^{d-l(d)-1} \gamma_S^{l(d)-1} r_d(\mathbf{a}^i) \quad [4]$$

301 with  $l(d)$  indexing the number of times a large loss outcome had been encountered  
 302 up to the point  $d$  in the sequence. That is, a probabilistic reduction in planning  
 303 beyond a large loss is captured by a lower continuing probability ( $\gamma_S$ ) after a large  
 304 loss.

305 Next, a “Loss sensitive” model with values  $Q^{\text{prune+LA}}(\mathbf{a})$  additionally allowed  
 306 the sensitivities to each of the outcomes  $r$  in equation 4 to be fitted separately for  
 307 every participant. For this model,  $\beta$  in equation 1 was fixed at unity. This ensured  
 308 that any aversive pruning was not simply due to a relatively stronger weighting of  
 309 losses compared to rewards (i.e. loss aversion (Tversky and Kahneman, 1991), the  
 310 well-known tendency for humans to overweight losses relative to gains of equivalent  
 311 magnitude).

312 Finally, we considered an additional Pavlovian attraction parameter that had  
 313 proved important in the behavioural study (Huys *et al.*, 2012). This captured the  
 314 attraction of states based on their average future consequences, irrespective of  
 315 whether sufficient choices remained on a trial to exploit those consequences. Most  
 316 critically, this captured participants’ tendency to move from state 6 to state 1 (-20p)  
 317 rather than to state 3 (+20p) when there was only one choice left in this state. We  
 318 found this effect in our current data too, with participants choosing the transition  
 319 from state 6 to state 1 on 53% of trials when only one choice remained, despite the  
 320 relative 40p cost entailed. However, there were fewer such trials in the current  
 321 version of the task, thus weakening its evidentiary basis.

322 The reader is referred to Huys *et al.* (2012) for a detailed discussion of these  
 323 models. The fitting procedures and the rationale for the group-level iBIC are also  
 324 discussed there.

325 Additional behavioural modelling was performed to generate parameter  
 326 estimates to approximate the aversive pruning on each particular trial, to include in  
 327 model-based fMRI analyses (O'Doherty *et al.*, 2007). As a marker for the engagement  
 328 of the neural circuits that are involved, we examined the inclination the subject had  
 329 to aversively prune on each trial, whether or not this behaviour actually occurred.  
 330 This inclination should depend on the trial type (being greater when there are more  
 331 opportunities for aversive pruning - e.g., on deeper trials) and should be higher the  
 332 stronger the individual's overall tendency to engage in aversive pruning. Short of a  
 333 validated process model for aversive pruning, we considered a surrogate measure of  
 334 trial- and subject-specific propensity that at least exhibits these two critical  
 335 properties. Specifically, we computed (using a set of parameters tailored to each  
 336 subject) two probability distributions over all possible sequences for every trial: first,  
 337 the distribution assuming that aversive pruning had no influence (i.e. fixing  $\gamma_S$  at  
 338 zero); and second, the distribution calculated using their fitted  $\gamma_S$ . The difference  
 339 between these two distributions, the Kullback-Leibler (KL) divergence, is our index of  
 340 the likely predilection to engage in aversive pruning on any given trial. Note that we  
 341 do not assume that subjects actually compute the distributions with and without  $\gamma_S$   
 342 – they are simply used here as a tractable proxy of the trial-by-trial variation in  
 343 inclination to engage in aversive pruning. The KL divergence was calculated between  
 344 the action distribution probability for models with and without aversive pruning. If  
 345  $p(\mathbf{a}|s_0, d, \gamma)$  is the probability of all possible action sequences of length  $d$  starting  
 346 from state  $s_0$  given by equation 3 (the Discount model, with only one  $\gamma$ ), and  
 347  $p(\mathbf{a}|s_0, d, \gamma_G, \gamma_S)$  is the same for equation 4 (the Pruning model, where  $\gamma$  is split),  
 348 the KL divergence  $D_{KL}$  is then:

$$349 \quad D_{KL} = \sum_{\mathbf{a}} p(\mathbf{a}|s_0, d, \gamma) \log \frac{p(\mathbf{a}|s_0, d, \gamma)}{p(\mathbf{a}|s_0, d, \gamma_S, \gamma_G)} \quad [5]$$

350 This KL divergence value was calculated for each successfully completed free  
 351 plan trial, including the training trials, and then Z-transformed such that the mean  
 352 was equal to zero and the standard deviation equal to 1 for each individual.  
 353 Importantly, the summed KL divergence value across trials for each participant was  
 354 highly correlated with the difference between their  $\gamma_G$  and  $\gamma_S$  values ( $r_{(37)} = 0.74$ ,  $P <$   
 355  $0.001$ ). Note that the KL divergence measure should be high on trials where the  
 356 possibility of aversive pruning is likely to have influenced subjects' behaviour to a  
 357 greater degree (e.g. with increased complexity), given their estimated overall  
 358 tendency to engage in aversive pruning.

359

### 360 MRI data acquisition

361 Brain images were acquired using a Siemens 1.5 Tesla Avanto MRI scanner with a 32-  
 362 channel sense head coil at the Birkbeck-UCL Neuroimaging Centre.

363 The task was presented via a head coil mirror and a front-of-bore projection  
 364 system. Two hundred and twenty-five T2\* weighted echo-planar imaging (EPI)

## Neural Basis of Aversive Pruning

365 volumes (42 slices per volume, slice repetition time (TR) = 87 ms, volume TR = 3.654  
366 s, echo time (TE) = 50 ms, slice tilt =  $-30^\circ$ , flip angle =  $90^\circ$ , field of view = 192 mm)  
367 were collected per run. The EPI sequence used was optimized to reduce signal  
368 dropout in both orbitofrontal cortex and amygdala regions (Weiskopf *et al.*, 2006).  
369 Phase oversampling (12%) was applied. Slices were positioned to maximally  
370 encompass ventral prefrontal and subcortical regions as these included our *a priori*  
371 hypothesized regions of interest (ROIs). Following task completion, field maps (short  
372 TE = 10 ms, long TE = 14.76 ms) were acquired in order to assess the inhomogeneity  
373 of the magnetic field. Finally, a 3D T1-weighted anatomical scan (magnetization  
374 prepared rapid gradient echo; 176 slices; slice thickness = 1 mm; gap between slices  
375 = 0.5 mm; TR = 2,730 ms; TE = 3.57 ms; field of view =  $256 \times 256$  mm<sup>2</sup>; matrix size =  
376  $256 \times 256$ ; voxel size =  $1 \times 1 \times 1$  mm resolution) was acquired at the end of each  
377 scanning session.

378

379 **fMRI preprocessing**

380 EPIs were pre-processed prior to analysis using Statistical Parametric Mapping (SPM)  
381 8 (release 4010; [www.fil.ion.ucl.ac.uk/spm](http://www.fil.ion.ucl.ac.uk/spm)) in MATLAB (7.1; Natick, MA). The first  
382 three volumes from each run were discarded to allow for T1 equilibrium effects,  
383 leaving 222 volumes per run. Images were spatially realigned to the fourth volume of  
384 the session and unwarped (using field maps), in order to correct for motion and  
385 geometric distortions caused by inhomogeneities in the magnetic field, respectively.  
386 Volumes corrupted due to movement (0.01% of all volumes) were excluded and  
387 replaced by linear interpolation of the surrounding images. Images were then  
388 normalized to Montreal Neurological Institute (MNI) co-ordinate space and  
389 smoothed with a Gaussian kernel of 4 mm full-width at half-maximum (FWHM).

390

391 **fMRI statistical analyses**

392 All fMRI analyses were conducted using SPM.

393 **First-level modelling**394 *Model-based fMRI – aversive pruning*

395 We first constructed an fMRI model to explore the impact of aversive pruning on  
396 planning on a trial-by-trial basis using the computationally derived KL divergence  
397 estimates, Z-transformed within each subject (i.e. model-based fMRI). In this model,  
398 all valid free plan trials were included in a single regressor, which was modulated  
399 first by difficulty (i.e. the number of sequences to evaluate;  $2^d = 8, 16$  or  $32$  for 3-, 4-  
400 and 5-move problems, respectively, where  $d =$  depth), to account for the linear  
401 effects of the expanding tree upon the KL divergence value. The difficulty-modulated  
402 regressor was then parametrically modulated by the KL divergence value. This, and  
403 all other models (except the model examining value itself), contained a separate  
404 parametric regressor representing the net monetary outcome of the chosen  
405 sequence across all trials (also time-locked to the planning period with the same  
406 duration). Specifically, the linear effect of anticipated reward on planning-related  
407 responses was modelled via a parametric regressor, with magnitude proportional to  
408 the net outcome provided by the chosen sequence. The inclusion of such a regressor

## Neural Basis of Aversive Pruning

409 removes value-related response variance from the analysis; this is important  
410 because aversive pruning is, by definition, monetarily disadvantageous. We also  
411 examined the effect of depth on KL divergence-related responses by computing the  
412 interaction of the KL divergence value and difficulty (again,  $2^d$ ) and entering it as a  
413 third parametric modulator.

414 *Distinguishing aversive pruning from planning and value-related networks*

415 In order to confirm established findings and the distinctiveness of our aversive  
416 pruning fMRI results from other networks and processes elicited by the task, we also  
417 constructed further models testing for the neural effects of planning and valuation.  
418 To examine responses related to difficulty during complex planning, we examined  
419 the first parametric modulator (difficulty:  $2^d$ ), which modulated the regressor  
420 containing all successfully completed free plan trials (time-locked to the planning  
421 period with the same duration (9 s)). The aim here was to locate the regions of the  
422 brain that scaled with the increasing cognitive demands of planning in our task. We  
423 constructed an additional model to explore outcome value-related networks. This  
424 value model contained a further parametric modulator time-locked to the outcome  
425 phase (2.4-4 s following the end of response input), which allowed us to examine  
426 value-related responses during both the planning and outcome phases (each in a  
427 separate regressor); we parametrically modulated the relevant portions of the trial  
428 by the net monetary outcome of each trial.

429 *Trial-based fMRI – aversive pruning*

430 For the trial-based fMRI analyses, the subject-level design matrix included separate  
431 regressors for the different trial types (defined according to participants' in-scanner  
432 choices - see "Basic behavioural analyses" above and Table 1) corresponding to the  
433 planning phase of the task. The following regressors of interest were included: OLL  
434 correct; ONLL correct; aversive pruning; OLL error; correct restricted plan large loss;  
435 and correct restricted plan no large loss. ONLL error trials were not included due to  
436 low trial numbers for this category and were included in a separate regressor of no  
437 interest. To model increasing cognitive demands with increasing depth, we entered  
438 trial difficulty as a parametric modulator. This parametric regressor on OLL correct,  
439 ONLL correct, aversive pruning, and OLL error entailed a modulation by the number  
440 of sequences that needed to be evaluated (i.e. difficulty,  $2^d$ ). Contrasting conditions  
441 parametrically modulated by depth should yield a more sensitive analysis of neural  
442 responses as the likelihood of aversive pruning grows with the branching or  
443 complexity of the decision tree.

444 *Model- and trial-based fMRI*

445 For both model-based and trial-based fMRI analyses, we also included regressors to  
446 model the response input phase (duration 2.5 s, in a single regressor for all trials)  
447 and outcome phase (duration 2.4-4 s). The outcome phase was categorised into the  
448 same six regressors as the planning phase for the trial-based fMRI analysis (free plan:  
449 OLL correct, ONLL correct, aversive pruning and OLL error; restricted plan: correct  
450 restricted plan large loss and correct restricted plan no large loss), again separately  
451 modelling the linear effect of net outcome across trial types. Additionally, to assess  
452 the impact of receiving a large loss, we contrasted OLL and ONLL correct trials during  
453 the outcome phase of the task. For both the model- and trial-based fMRI analyses,



454 regressors of no interest included missed/no-response trials, ONLL error trials and  
455 incorrect restricted plan trials combined into a single regressor (whole-trial duration:  
456 16 s), as well as regressors modelling null scans for the two scans immediately  
457 before and after the second run, and interpolated images following removal of  
458 corrupted scans (if any). Fixation trials were not modelled explicitly and constituted  
459 an implicit baseline. The six realignment parameters were also included in the  
460 model. All regressors were modelled as boxcars time-locked to the trial phase  
461 (planning, input, and outcome) with the corresponding duration (9 s, 2.5, and 2.4-4  
462 s, respectively), and convolved with SPM's canonical hemodynamic response  
463 function.

464 Estimation incorporated a high-pass filter at 1/128 Hz and serial correlations  
465 intrinsic to the fMRI time series were accounted for using an AR(1) model. The three  
466 runs were modelled as a single concatenated run to avoid non-estimation of entire  
467 runs for participants with low numbers of event types.

468

#### 469 **Second-level modelling**

470 Following estimation, subject-level contrast images were smoothed with a 7 mm  
471 FWHM kernel, and entered into group-level one-sample *t*-tests. Activations were  
472 localized with reference to the group-averaged anatomical scan and the atlas of Mai  
473 and colleagues (2003). Given our *a priori* hypotheses regarding the neural basis of  
474 aversive pruning (Dayan and Huys, 2008), we applied an initial threshold of  $P = 0.005$   
475 and applied family-wise error (FWE) correction for multiple comparisons at the  
476 voxel-level, adjusted for small volume (SVC) across our ROIs. For the planning phase  
477 analysis, the SGC ROI was defined as an 8 mm box centred on of the peak coordinate  
478 from a study reporting altered glucose metabolism in patients with depression (MNI  
479 coordinates, [ $x = -2$ ,  $y = 32$ ,  $z = -2$ ]; (Drevets *et al.*, 1997)). The PAG ROI was defined  
480 as an 8 mm box centred on the peak coordinate previously identified as activating to  
481 increasing threat using fMRI in healthy human participants (MNI coordinates, [ $x = -$   
482  $3$ ,  $y = -25$ ,  $z = -11$ ] (Mobbs *et al.*, 2007). A bilateral amygdala ROI was created from  
483 the Wake Forest University (WFU) Pickatlas toolbox for SPM  
484 (<http://www.fmri.wfubmc.edu/download.htm>) with the Automated Anatomical  
485 Labelling atlas. We anticipated very robust responses for the more general planning  
486 and value-related networks; thus, for the purposes of inference, outside our ROIs,  
487 we increased our threshold such that only voxels surviving whole-brain voxel-level  
488 FWE correction  $< 0.05$  survived. All second-level analyses incorporated an explicit  
489 binary grey matter mask.

490 For the trial-based analyses, the main contrasts we report are derived from  
491 linear combinations of the ONLL correct, OLL correct and aversive pruning  
492 regressors, which are comparable in terms of visual input during the planning and  
493 outcome phases, and the correct restricted plan trials. Since trials were categorised  
494 according to participants' decisions, some participants had fewer than four trials in a  
495 given condition; these participants were excluded from the relevant contrasts,  
496 resulting in slightly different numbers of subjects across analyses. For the outcome  
497 phase analysis, we anticipated that activation in the insula would be elicited during  
498 the receipt of large losses (Garrison *et al.*, 2013). Therefore, for this analysis we

## Neural Basis of Aversive Pruning

499 created a bilateral insula ROI from the WFU Pickatlas and applied SVC as described  
500 above.

501 For the trial-based planning analyses our primary contrast of interest was the  
502 comparison of aversive pruning trials (on which participants avoided the optimal  
503 sequence that contained a large loss and instead chose the best available large-loss-  
504 free sequence), relative to OLL correct trials (on which participants chose an optimal  
505 sequence transitioning through a large loss). To control for the effects of  
506 transitioning through a large loss *per se* on OLL correct trials we included the  
507 restricted plan trials to create the following contrast: aversive pruning + restricted  
508 plan large loss > OLL correct + restricted plan no large loss. We ensured that  
509 difficulty was matched across this contrast by selecting trials that provided an equal  
510 ratio of 3:4:5 move problems for each participant across the aversive pruning and  
511 OLL correct conditions. For restricted plan trials, the inclusion threshold was set at  
512 chance level (50%); two participants failed to meet this criterion due to a failure to  
513 understand trial instructions and were excluded from analyses including this trial  
514 type. To control for possible difficulty differences between restricted plan trials,  
515 (because there were more divergent arrows in the restricted plan large loss  
516 condition), trials were chosen to match the number of divergent arrows between the  
517 two restricted plan trial types.

518 Finally, we constructed additional contrasts to test how the above planning  
519 contrasts were modulated by difficulty ( $2^d$ ). These contrasts are derived from linear  
520 combinations of the OLL correct, ONLL correct and aversive pruning parametric  
521 modulator regressors, but exclude the restricted plan trials; the latter are  
522 unnecessary here as the parametric modulator already entails a contrast (between  
523 more difficult and easier trials) within each condition, controlling for the transition  
524 through the large loss *per se* on OLL correct trials. As above, three main contrasts  
525 were examined: 1) aversive pruning parametric modulator > OLL correct parametric  
526 modulator; 2) OLL correct parametric modulator > ONLL correct parametric  
527 modulator; and 3) ONLL correct parametric modulator > aversive pruning parametric  
528 modulator.



529 **Results**

530 We describe two broad collections of behavioural analysis, and through this,  
 531 associated fMRI responses. Following a brief description of the broad patterns of  
 532 behaviour observed on the task, which paralleled our previous findings (Huys et al.,  
 533 2012) we initially consider a computational model-based treatment that aimed to  
 534 characterize the whole structure of behaviour using a parsimonious model whose  
 535 parameters are intended to capture the general tendencies of each subject. Imaging  
 536 analyses associated with this model duly indicated the general architecture of  
 537 control. We then explore the specificity of our imaging analyses in the context of  
 538 other known neural architecture underlying the cognitive components implicated in  
 539 our task. Finally, for completeness, we provide complementary behavioural and fMRI  
 540 analyses based on categorisations of trials (see Table 1).

541 **Behavioural and modelling evidence for pruning**

542 Participants chose the correct sequence on average 78% (SD = 18%) of the time on  
 543 free plan trials on which the optimal sequence did not include a large loss (ONLL); on  
 544 these trials aversive pruning would not be disadvantageous. By contrast, on free plan  
 545 trials on which the optimal sequence did include a large loss (OLL), for which  
 546 aversive pruning would be disadvantageous, performance was impaired for every  
 547 participant (mean OLL correct = 37% (SD = 18%)). The difference between  
 548 performance on these trial types was substantial and highly significant (mean  
 549 difference = 41% (SD = 20%),  $t_{(36)} = 12.51$ ,  $P < 0.001$ ,  $d = 2.06$ ; **Figure 2A**), confirming  
 550 our previous findings (Huys et al., 2012). As expected, performance also became  
 551 worse with increasing difficulty ( $F_{(2,72)} = 132.75$ ,  $P < 0.001$ ,  $\eta_p^2 = 0.787$ ; **Figure 2B**), but  
 552 remained high even for depth 5 choices, where there are 32 different paths.  
 553 Critically, there was a significant interaction between trial type and difficulty ( $F_{(2,72)} =$   
 554  $5.58$ ,  $P = 0.009$ ,  $\eta_p^2 = 0.134$ ). Planned contrasts revealed that the requirement to  
 555 transit through a large loss to attain the optimal amount had an increasingly  
 556 detrimental effect on decision-making at higher difficulty (depth 3: mean difference  
 557 = 34% (SD = 25%),  $t_{(36)} = 8.26$ ,  $P < 0.001$ ,  $d = 1.36$ ; depth 4: mean difference = 40%  
 558 (SD = 22%),  $t_{(36)} = 11.29$ ,  $P < 0.001$ ,  $d = 1.86$ ; depth 5: mean difference = 49% (SD =  
 559 29%),  $t_{(36)} = 10.33$ ,  $P < 0.001$ ,  $d = 1.70$ ). Note, though, that this analysis does not  
 560 examine where the loss appeared in the tree.

561 **Figure 2 about here**562 **Model-based aversive pruning behaviour and associations with psychometric variables**

563 Consistent with our previous report (Huys *et al.*, 2012), there was substantial  
 564 evidence for aversive pruning based on our computational model (see **Figure 2C-D**;  
 565 Pruning and Pruning+Loss models). That is, the most parsimonious model (smallest  
 566 negative model evidence iBIC; red star in **Figure 2E**; see **Table 2** for model  
 567 performance overview) incorporated aversive pruning, with steeper discounting  
 568 after large losses than after other outcomes ( $\gamma_G$  is significantly larger than  $\gamma_S$ ,  $t_{(36)} =$   
 569  $5.12$ ,  $P < 0.001$ ,  $d = 0.84$ ; **Figure 2F**; improvement in  $\log_{10}$  model evidence between  
 570 model Discount and model Pruning ( $\Delta$ iBIC) = 77.5, indicative of decisive evidence in  
 571 favour of the Pruning model). Loss aversion was also evident (**Figure 2G**), such that  
 572 the best model incorporated fitted reward and loss sensitivities ( $\Delta$ iBIC between

573 model Pruning and Pruning+Loss) = 5.8). It is important to distinguish between these  
 574 two loss-related processes that are included in our model. Aversive pruning, as  
 575 instantiated in the model, is not simply a discounting of the value associated with  
 576 transitions (or subsequent paths). Instead, the aversive pruning parameter controls  
 577 whether paths following large losses are actually explored at all, regardless of the  
 578 possible gains that lie behind them. We consider such a reflexive avoidance of even  
 579 considering options to be Pavlovian in nature, as it is elicited automatically and not  
 580 related to the overall value of the path. Excessive discounting of the value of  
 581 negative transitions (equivalent to loss aversion) does occur in our data, but this is  
 582 controlled by a different set of parameters and is conceptually separate from  
 583 pruning.

584 Importantly, our computationally-derived general planning parameter ( $\gamma_G$ )  
 585 was positively correlated with its trial-based equivalent (ONLL percent correct:  $r_{(37)} =$   
 586  $0.73$ ,  $P < 0.001$ ; **Figure 2H**). The difference between OLL and ONLL percent correct  
 587 was strongly correlated with the equivalent metric derived from the computational  
 588 analyses ( $\gamma_G - \gamma_S$ :  $r_{(37)} = 0.63$ ,  $P < 0.001$ ; **Figure 2I**), providing convergent validity for the  
 589 two approaches. However, due to the uncertainty attached to both choice frequency  
 590 and model parameter estimates this correlation is not perfect and some subjects  
 591 with small or even negative difference between  $\gamma_S$  and  $\gamma_G$  still show a positive  
 592 difference between ONLL and OLL frequencies. It would be interesting to examine  
 593 subjects who do and do not show aversive pruning separately, or indeed look for  
 594 changes over time in the strength of pruning. Unfortunately, the present sample size  
 595 does not allow for this; therefore, we concentrate here on correlational analyses.  
 596 Finally, further validation of the model comes from sampling surrogate data (Figure  
 597 2J-L).

598 Overall, these results are consistent with our previous report in an  
 599 independent sample (Huys *et al.*, 2012), and provide complementary evidence for  
 600 the presence of aversive pruning. The slow degradation of performance with depth  
 601 on the ONLL trials is compatible with the fact that the number of trials without a  
 602 large loss increases slowly with depth, and that aversive pruning allows the  
 603 concentration of resources on these paths.

604

605 **Table 2.** Model performance values

Model	Number of parameters	Choice log likelihood	% variance explained	iBIC
Pruning + Loss	6	1151	55.3	2466
Pruning	3	1173	54.4	2472
Discount	2	1221	52.5	2549
Lookahead	1	1502	41.7	3052

606

607 iBIC: integrated Bayesian information criteria

608 A multiple regression analysis revealed that state anxiety, but no other  
 609 included variable (IQ, gender, age, depression and trait anxiety), correlated with the  
 610 difference between ONLL and OLL percent correct ( $t_{(37)} = 2.12$ ,  $P = 0.042$ ); variance  
 611 inflation factor (VIF) values were less than 3.0 for all independent variables,

612 suggesting an adequate lack of collinearity. Contrary to our expectations, however,  
 613 no psychometric variables correlated with the computationally derived aversive  
 614 pruning estimate ( $\gamma_G - \gamma_S$ ). In particular, we did not replicate our previous finding that  
 615 this statistic was correlated with subclinical depression scores, though we note that  
 616 the range of scores in the present study was relatively low.

#### 617 **Aversive pruning recruits the subgenual cingulate cortex**

618 We used the computational model to construct, separately for each participant's  
 619 maximum *a posteriori* parameters, a measure of the inclination to engage in aversive  
 620 pruning on each trial. This is the Kullback-Liebler (KL) divergence between the  
 621 distributions of trajectories assuming discounting based on depth alone (discount  
 622 model) vs discounting based on losses encountered (pruning model). **Figure 3A**  
 623 confirms that the KL divergence increases with depth ( $F_{(2, 72)} = 223.82$ ,  $P < .001$ ,  $\eta_p^2 =$   
 624  $0.86$ ), with all three groups significantly different from each other,  $P < 0.001$ ), as  
 625 expected from the likely extra opportunities for aversive pruning with longer  
 626 sequences. **Figure 3B** shows that the measure was indeed higher on aversive pruning  
 627 trials (based on participant choices – see Table 1); however, there were no  
 628 significant differences between trial types ( $F_{(3, 108)} = 0.74$ ,  $P = 0.48$ ,  $\eta_p^2 = 0.02$ ).  
 629 Negative KL divergence values shown here arise due to the mean correction applied  
 630 to the metric used for fMRI analyses.

631 We entered the KL divergence value on each trial as a parametric regressor  
 632 across all successfully completed free plan trials, controlling for difficulty (which was  
 633 entered as the first parametric regressor) and trial net value. Consistent with our  
 634 primary hypothesis, this analysis revealed that SGC activation increased with our  
 635 metric of inclination to engage in aversive pruning, the KL divergence ( $[x = -6, y = 29,$   
 636  $z = -2]$ ;  $t_{(36)} = 3.87$ ,  $P_{SVC} = 0.004$ ; **Figure 3C**). The interaction between KL divergence  
 637 and difficulty also revealed a greater modulation of SGC activation by inclination to  
 638 engage in aversive pruning at higher depth ( $[x = -6, y = 35, z = -5]$ ;  $t_{(36)} = 3.47$ ,  $P_{SVC} =$   
 639  $0.009$ ; **Figure 3D**).

640 In summary, our computational fMRI analyses revealed that SGC activation  
 641 was higher on trials on which our model indicated that there was a greater  
 642 inclination to indulge in aversive pruning, and this was particularly the case on more  
 643 difficult trials. In the following analyses we show that this activation in the SGC is  
 644 separate to responses related to planning and valuation.

#### 645 **Figure 3 about here**

#### 646 **Planning and valuation responses**

647 We next explored the specificity of our aversive pruning results relative to other  
 648 neural networks known to be associated with cognitive processes required during  
 649 successful undertaking of our task, namely planning and valuation. We first explored  
 650 the effect of planning by examining the first parametric modulator, which indexed  
 651 difficulty ( $2^d$ ). As expected, increasing difficulty robustly activated a network of  
 652 regions identified in previous studies of planning. This included the bilateral dorsal  
 653 cerebellum, primary visual, supplementary motor, and DLPFC, thalamus, dorsal  
 654 caudate and putamen, all of which survived whole-brain (WB) voxel-level correction  
 655 for multiple comparisons (all  $t_{(36)} > 5.45$ ,  $P_{WB} < 0.05$ ; **Figure 4A**).

656 To examine responses related to receipt of outcomes, we constructed a  
 657 separate model in which the net monetary value of the chosen sequence was  
 658 entered as a parametric regressor, time-locked to the outcome period. Increasing  
 659 monetary outcome robustly activated the VS (left [ $x = -12, y = 8, z = -8$ ];  $t_{(36)} = 7.74$ ,  
 660  $P_{WB} < 0.001$ ; right [ $x = 12, y = 8, z = -8$ ];  $t_{(36)} = 5.52$ ,  $P_{WB} = 0.027$ ; **Figure 4B**, left panel),  
 661 the medial orbitofrontal cortex (mOFC; [ $x = 0, y = 44, z = -14$ ];  $t_{(36)} = 5.88$ ,  $P_{WB} =$   
 662  $0.013$ ; **Figure 4B**, middle panel), and the head of the caudate ([ $x = -6, y = 20, z = 7$ ];  
 663  $t_{(36)} = 7.17$ ,  $P_{WB} < 0.001$ ; **Figure 4B**). Given the wealth of research establishing the  
 664 existence of value signals in the VS and OFC (Schultz, 2015), we correlated the large  
 665 reward (+140p) sensitivity parameter from our winning computational model with  
 666 the net outcome-related activation at the peak voxel within these regions. This was  
 667 significant in the mOFC ( $r_{(37)} = 0.46$ ,  $P = 0.004$ ; **Figure 4B**, right panel), but not the VS  
 668 ( $r_{(37)} = 0.13$ ,  $P = 0.45$ ).

669

**Figure 4 about here**

### 670 **Neural response to large losses is associated with aversive pruning tendency**

671 During the outcome phase, participants would no longer have any reason to plan,  
 672 but instead had just to observe their executed plan being replayed with feedback on  
 673 the monetary consequence of each box-to-box move. We next asked whether the  
 674 tendency to engage in aversive pruning might impact on activation during this phase.  
 675 To do this, we examined trials on which volunteers could have aversively pruned but  
 676 (correctly) chose not to. Thus, again controlling for net objective outcome, we  
 677 compared trials on which subjects correctly avoided aversively pruning, therefore  
 678 receiving at least one large loss during the entire sequence (OLL correct), with  
 679 correct trials that avoided all large losses (i.e. aversive pruning was helpful, ONLL  
 680 correct) (note that all of the trials in this contrast involved optimal decisions).

681 This contrast revealed activation in our insula ROI ( $[x = 33, y = 23, z = -5]$ ;  $t_{(36)}$   
 682  $= 4.70$ ,  $P_{SVC} = 0.011$ ; **Figure 4C**, left panel), as well as robust responses that survived  
 683 whole-brain correction in the inferior parietal lobule (IPL; [ $x = 39, y = -52, z = 46$ ];  $t_{(36)}$   
 684  $= 4.78$ ,  $P_{WB} = 0.01$ ) and DLPFC [ $x = 45, y = 44, z = 4$ ];  $t_{(36)} = 4.32$ ,  $P_{WB} < 0.001$ ). We next  
 685 asked whether the tendency to engage in aversive pruning might be related to  
 686 activation to the receipt of large losses (**Figure 4C**, middle panel). Activation in the  
 687 insula ( $r_{(37)} = 0.47$ ,  $P = 0.003$ ; **Figure 4C**, right panel) and DLPFC ( $r_{(37)} = 0.35$ ,  $P =$   
 688  $0.034$ ), but not in IPL ( $r_{(37)} = 0.22$ ,  $P = 0.20$ ), correlated significantly with our  
 689 computationally derived measure of aversive pruning,  $\gamma_G - \gamma_S$  (although the  
 690 correlations between activation in the insula ( $Z = 1.58$ ,  $P = 0.113$ ) and DLPFC ( $Z =$   
 691  $0.85$ ,  $P = 0.39$ ) and aversive pruning behaviour were not significantly greater than  
 692 that in the IPL).

693

### 694 **Confirmatory trial-based behavioural and fMRI analyses**

#### 695 **Trial-based behaviour provides further evidence of pruning**

696 Further evidence consistent with aversive pruning comes from a finer classification  
 697 of suboptimal choices. Of course, it is not possible to be definitive as to the  
 698 processes that underlie any particular suboptimal (or indeed optimal) choice.  
 699 However, trials for which it would have been optimal to transition through a large

700 loss, but participants selected the best available option that avoided large losses  
701 (e.g. **Figure 1B**) are at least suggestive of aversive pruning-influenced planning. We  
702 call these aversive pruning trials. All other instances of suboptimal selection we term  
703 as errors (separated into trials for which the optimal decision entailed (OLL error;  
704 excluding aversive pruning trials, i.e. this category did not include trials where the  
705 next best available option that did not entail transitioning through a large loss was  
706 chosen) or avoided (ONLL error) transitioning through a large loss: see Table 1). Due  
707 to low trial numbers ONLL errors were not considered further.

708 A clear example of aversive pruning occurs in the scenario depicted in **Figure**  
709 **5A**. Placed in state 2 with 3 moves to plan, the optimal solution is to go from state 2  
710 to state 5 (-70p), from state 5 to state 1 (-70p) and from state 1 back to state 2  
711 (reaping the only large reward in the maze: +140p). This sequence results in breaking  
712 even, and participants chose it 41% (SD = 33%) of the time (**Figure 5A**, blue  
713 outcome). However, in spite of the relative ease of the problem (only 8 sequences  
714 needed evaluating), participants had a strong tendency to engage in aversive  
715 pruning, presumably because the optimal sequence contains two large losses. The  
716 best available option that avoided the large loss involved moving from state 2 to  
717 state 3 (-20p), from state 3 to state 4 (-20p), and from state 4 back to state 2 (+20p)  
718 (resulting in a net loss of 20 pence). Such aversive pruning arose on 37% (SD = 31%;  
719 aversive pruning percentage) of trials (**Figure 5A**, red outcome), i.e., nearly as often  
720 as the optimal choice. By way of comparison, subjects selected the optimal and the  
721 next best available sequence 80% (SD = 23%) and 14% (SD = 20%) of the time,  
722 respectively, on the ONLL trial requiring 3 moves to plan from state 5.

723 Participants displayed a strong tendency towards aversive pruning, choosing  
724 the best sequence that avoided a large loss on around 52% (SD = 23%) of OLL trials in  
725 which they chose suboptimally (chance = ~11% across depths). All subjects engaged  
726 in aversive pruning, however the extent of the predilection was highly variable  
727 across the sample (4-93%); nevertheless, the aversive pruning percentage was very  
728 consistent within subjects between the 1<sup>st</sup> and 2<sup>nd</sup> half of the trials ( $r_{(37)} = 0.69$ ,  $P <$   
729  $0.001$ ). Interestingly this fraction, which we call the aversive pruning percentage, did  
730 not depend on depth ( $F_{(2,72)} = 1.15$ ,  $P = 0.32$ ,  $\eta_p^2 = 0.03$ ; **Figure 5B**), thus supporting  
731 the hypothesis that aversive pruning acts as an adaptive heuristic to reduce the  
732 number of options to be considered, allowing participants to maintain reasonable, if  
733 not perfect, planning performance across depths (Huys *et al.*, 2012). We also  
734 examined the average earnings, which revealed a significant main effect of trial type  
735 (**Figure 5C**;  $F_{(3,108)} = 320.538$ ,  $P < .001$ ,  $\eta_p^2 = 0.90$ ). Perhaps surprisingly, aversive  
736 pruning choices earned participants significantly more money than OLL correct  
737 choices ( $t_{(36)} = 6.74$ ,  $P < 0.001$ ,  $d = 1.11$ ). Although by definition optimal choices  
738 would have earned more on aversive pruning trials (**Figure 5C**, light red bar; mean  
739 difference = 33p, SD = 9p), this pattern arises because aversive pruning occurred  
740 more frequently with increasing depth (while OLL correct trials were rarer to be  
741 performed at higher depth), and the average net value largely increases with depth  
742 (OLL correct: depth 3 = 33p, depth 4 = 67p, depth 5 = 93p; aversive pruning: depth 3  
743 = -20p, depth 4 = 13p, depth 5 = 50p; OLL error: depth 3 = -84p, depth 4 = -59p,  
744 depth 5 = -47p) (although this is not the case for ONLL correct trials (depth 3 = 100p,  
745 depth 4 = 80p, depth 5 = 60p)).



746 If aversive pruning is indeed a heuristic that reduces the number of evaluated  
 747 sequences, then we might see an effect on reaction times (RT: **Figure 5D**; note  
 748 though, that subjects could not enter choices until the 9s of planning had elapsed,  
 749 which could reduce the magnitude of this effect). There was a main effect of trial  
 750 type (Friedman  $\chi^2(3) = 33.876$ ,  $P < 0.001$ ). Post-hoc tests revealed that ONLL correct  
 751 RTs were significantly shorter than OLL correct RTs ( $Z = 2.105$ ,  $P = 0.035$ ) and  
 752 aversive pruning RTs ( $Z = 4.413$ ,  $P < 0.001$ ). However, contrary to our expectations,  
 753 the difference in RT between OLL correct and aversive pruning choices was non-  
 754 significant ( $Z = -1.335$ ,  $P = 0.182$ ). Nevertheless, aversive pruning choices were made  
 755 significantly faster than OLL error trials ( $Z = 2.844$ ,  $P = 0.004$ ).

756 Finally, we note that the difficulty in planning transitions through large losses  
 757 was even evident on the much easier restricted plan trials (on which only two  
 758 sequences required evaluation). Participants made the optimal choice significantly  
 759 more often on restricted plan trials that did not feature large losses (mean = 90%, SD  
 760 = 9%) than on those that did (mean = 84%, SD = 8%;  $t_{(34)} = 3.74$ ,  $P < 0.001$ ,  $d = 0.63$ ).  
 761 However, there was no effect on RT (correct trials only:  $t_{(34)} = 1.12$ ,  $P = 0.27$ ,  $d =$   
 762  $0.19$ ).

763 **Figure 5 about here**

#### 764 **Trial-based fMRI confirms a role for the SGC in aversive pruning**

765 A contrast between aversive pruning and OLL correct trials during the planning  
 766 period (incorporating restricted plan control trials, controlling for net outcome;  
 767  $N=31$ ) revealed no significant activation in our ROIs, and no cluster survived whole-  
 768 brain correction for multiple comparisons. However, an analysis of the parametric  
 769 modulation of aversive pruning trials by difficulty (contrasted against the parametric  
 770 modulation of OLL correct trials by difficulty, again controlling for net income:  $N=33$ )  
 771 revealed a cluster in the SGC extending into pregenual ACC ( $[x = -3, y = 35, z = -2]$ ;  
 772  $t_{(32)} = 3.08$ ,  $P_{SVC} = 0.023$ ; left panel of **Figure 5E**). We also note the presence of a  
 773 cluster in the right amygdala, though this did not survive correction for multiple  
 774 comparisons and therefore we do not consider it further ( $[x = 21, y = 2, z = -20]$ ;  $t_{(32)} =$   
 775  $2.85$ ,  $P_{SVC} = 0.144$ ). The result in the SGC was driven by a progressive reduction in  
 776 response with increasing difficulty on OLL correct trials (i.e. a negative modulation by  
 777 difficulty; one-sample  $t$ -test against zero:  $t_{(32)} = 3.72$ ,  $P = 0.001$ ), while difficulty did  
 778 not affect activation on aversive pruning trials ( $t_{(32)} = 1.09$ ,  $P = 0.285$ ; right panel of  
 779 **Figure 5E**). This finding that aversive pruning elicits a (relative) increase in SGC  
 780 activation as depth increases, complements the one arising in our computationally-  
 781 motivated analysis based on the KL divergence, where a robust modulation by  
 782 difficulty was also identified. Taken together, these results suggest that inhibiting  
 783 aversive pruning may require deactivation of the SGC, particularly when decisions  
 784 are more complex.

785 None of our other comparisons yielded significant activation in our ROIs, or  
 786 activation in other regions that survived whole-brain correction for multiple  
 787 comparisons. Contrasting the parametric effect of difficulty between aversive  
 788 pruning and ONLL correct trials ( $N=35$ ) did not reveal any effect surviving correction  
 789 for multiple comparisons. The equivalent parametric contrast between ONLL and

Neural Basis of Aversive Pruning

790 OLL correct trials (N=35) revealed an effect in the right amygdala that narrowly  
791 missed significance ( $[x = 33, y = -1, z = -20]$ ;  $t_{(34)} = 3.25, P_{SVC} = 0.062$ ).



792 **Discussion**

793 Multi-step decision-making is fundamental to human behaviours. However, fully  
794 solving complex planning problems is often too arduous, thus necessitating  
795 heuristics. We used a combination of neuroimaging and computational modelling of  
796 behaviour to characterise the neural basis of one such simple approximation,  
797 aversive pruning. This is the inflexible, reactive curtailment of search when a large  
798 loss is encountered during planning. Aversive pruning represents a computationally  
799 well-defined influence of a Pavlovian inhibitory response on high-level cognitive  
800 manipulations during planning. We replicated previous findings that aversive pruning  
801 was ubiquitous across subjects (Huys *et al.*, 2012). As expected, it served to preserve  
802 computational resources, being more prevalent on harder problems, and was  
803 associated with faster responses than other suboptimal decisions. Both  
804 computational model- and trial-based neuroimaging analyses showed that aversive  
805 pruning was associated with haemodynamic responses in the SGC during planning.  
806 By contrast, distinct circuits were activated by planning and valuation. Further, the  
807 responses to the receipt of large losses in the insula and DLPFC correlated with one  
808 of our computationally-derived behavioural measures of overall aversive pruning.  
809 Our results reveal the neural and computational architecture underlying a  
810 profoundly influential heuristic that enables humans to make complex planned  
811 decisions with reasonable speed and accuracy.

812 The aversive pruning-related activation that we identified in the SGC through  
813 both computational and categorical analyses exists over and above planning- and  
814 value-related responses. Closer examination of the parametric modulation by  
815 difficulty sheds further light on the nature of this finding. In comparison to correct  
816 decisions that transitioned through a large loss, aversive pruning was associated with  
817 higher SGC activation especially on more difficult problems. Intriguingly, our trial-  
818 based analyses suggest that this effect was largely driven by a relative decrease in  
819 SGC response on correct decisions that transitioned through a large loss as planning  
820 complexity increased (**Figure 5E**). This is consistent with studies examining the trade-  
821 off between appetitive and aversive outcomes. In humans, Talmi *et al.* (2009) also  
822 found SGC inhibition when participants chose to endure a punishment in order to  
823 obtain a gain. In non-human primates, Amemori and Graybiel (2012) reported that  
824 neurons in the homologous area of the ACC in the macaque (BA24b) responded to  
825 aversive stimuli in an approach-avoidance decision task; localized microstimulation  
826 of these neurons increased the negative impact of aversive consequences on choice.  
827 Thus, it appears that planning through a negative outcome in order to achieve an  
828 overall positive outcome is facilitated when the SGC is deactivated.

829 Importantly, the SGC is a key node where cognition and emotion are thought  
830 to interact pathologically, for example in mood disorders (Drevets *et al.*, 2008, Roiser  
831 *et al.*, 2012). The anatomical correspondence between resting-state findings in  
832 depressed patients, punishment-driven anticipatory responses in healthy humans,  
833 and aversive signals in non-human primates is striking. The SGC may be an important  
834 mediator of the inhibitory effect of aversive expectations not just on behaviour, but  
835 also on higher-level cognitive function in mood disorders. In the context of  
836 depression, it has been suggested that inhibitory control is impaired and that this  
837 underlies some of depressed subjects' inability to disengage from aversive

838 information (Dayan and Huys, 2008, Joormann and Gotlib, 2010). However, the SGC  
839 appears to be hyperactive during rumination, and in depression more generally  
840 (Cooney *et al.*, 2010), possibly suggesting a reduced efficiency of these mechanisms  
841 rather than a lack of engagement.

842         Complex decision-making processes recruit a diverse set of hierarchical  
843 cognitive components (Solway and Botvinick, 2012) and neural structures (Newman  
844 *et al.*, 2003). We note here at least two neural network processes on top of which  
845 aversive pruning occurs. First, planning a complex sequence of actions requires  
846 considerable cognitive control. Unsurprisingly, as planning difficulty increased in our  
847 task, structures such as the cerebellum, DLPFC, dorsal striatum, motor cortex, and  
848 thalamus were increasingly activated (**Figure 4A**). These brain regions are frequently  
849 implicated in planning tasks which require cognitive control (Newman *et al.*, 2003)  
850 and in goal-directed approaches to problem solving (Solway and Botvinick, 2012). A  
851 second important component process of decision-making is the evaluation of  
852 outcomes associated with action sequences. Increasing net monetary outcome was  
853 associated with activation in a network of structures commonly activated in  
854 reinforcement learning tasks and thought to underlie valuation, including the VS and  
855 the mOFC (Schultz, 2015). Interestingly, activation in mOFC, but not VS, at the time  
856 of outcome was associated with our computationally-derived behavioural measure  
857 of sensitivity to large reinforcements. This finding is consistent with the hypothesis  
858 that mOFC is critical for processing outcomes *per se*, while VS is more closely aligned  
859 with prediction error signalling (Schultz, 2015).

860         When we focused our analysis on the outcome phase (contrasting optimal  
861 decisions with and without large losses) we found that a number of regions (insula,  
862 IPL and DLPFC) were significantly more activated during the receipt of large losses,  
863 even after accounting for trial-by-trial monetary earnings. Even though the actual  
864 planning would have terminated before this point, activations in the structures that  
865 responded positively to large losses (insula and DLPFC) also correlated positively  
866 with our computationally derived estimate of overall aversive pruning ( $\gamma_G - \gamma_S$ ). Of  
867 particular relevance is the insula, which is thought to play a role in interoceptive  
868 perception and the production of subjective negative feeling states (Medford and  
869 Critchley, 2010), and has been reported to influence decision-making (Yu *et al.*,  
870 2010). For example, individuals with insula damage have been reported to exhibit a  
871 selective impairment in avoiding stimuli associated with monetary losses (Palminteri  
872 *et al.*, 2012). We had not predicted activation of DLPFC and IPL in the outcome  
873 phase, but this pattern would be consistent with the engagement of inhibitory  
874 processes during cognitive control (Guitart-Masip *et al.*, 2012). We speculate that  
875 these results may indicate a similar involvement in aversive pruning, though this  
876 needs to be tested in future studies. The activation of the DLPFC is particularly  
877 noteworthy with respect to depression. Fales and colleagues (2008) showed a failure  
878 to activate the DLPFC during suppression of irrelevant aversive information in  
879 depression. As aversive pruning might relate to the ability to inhibit the processing of  
880 aversive information, and hence correlate negatively with rumination (Gotlib and  
881 Joormann, 2010), a clear prediction is that a similar pattern would be observed when  
882 depressed patients aversively prune.

## Neural Basis of Aversive Pruning

883           Taking the above results together, a possible model accounting for our fMRI  
884 results is that the DLPFC and insula might co-ordinate to mark parts of the decision  
885 tree that contain large losses. Once the tree is demarcated, these signals may then  
886 be used during the planning phase where SGC responses drive the decision to prune.  
887 Meanwhile, deactivation of the SGC appears critical to choosing to engage with the  
888 large loss in order to make an optimal decision. The consistency of the SGC response  
889 between our computational and categorical fMRI analyses during planning supports  
890 the notion that this region participates in curtailing the decision tree search on  
891 encountering a large loss. Although we cannot directly exclude an additional causal  
892 influence, whereby it is the overloading of cognitive control that leads to the release  
893 of the pruning reflexes, the structure of the findings still argue for a shaping  
894 influence of the pruning reflexes on the process of evaluation.

895           A limitation of the current work is that the aversive pruning time-point(s)  
896 during planning are not clearly temporally delineated; we therefore cannot make  
897 temporal causality claims about the neural effect. Aversive pruning is a meta-  
898 reasoning process involving multiple repeated decisions about what to evaluate next  
899 (Russell and Wefald, 1991). The ambiguity surrounding the precise point at which  
900 aversive pruning occurs could be resolved more directly, possibly using a  
901 combination of eye-tracking and neuroimaging methods with higher temporal  
902 resolution such as EEG or MEG. A further limitation is that our study was performed  
903 in healthy participants and was not designed to detect correlations with symptoms  
904 of mood or anxiety disorders. In a previous study (Huys *et al.*, 2012) aversive pruning  
905 correlated with subclinical measures of depression, while in the current study, it  
906 correlated with state anxiety. We originally hypothesised (Dayan and Huys, 2008)  
907 that aversive pruning might relate to both symptoms of depression and anxiety  
908 because features of impaired inhibition of aversive processing are prominent in both  
909 disorders. The failure to confirm our previous finding of a correlation with depressive  
910 symptoms might be due to a restricted range of scores in the present sample.

911           In summary, it is tremendously difficult to plan optimally in complex  
912 problems; heuristics are frequently mandatory. We confirmed the pervasive  
913 influence of one such shortcut, aversive pruning, over goal-directed behaviour,  
914 distinguishing its impact from those of other decision-making biases. Our  
915 neuroimaging results revealed that aversive pruning recruits neural structures  
916 implicated in decision-making and mood disorders, specifically the SGC. DLPFC and  
917 insula responses to large losses and anxiety levels, an established risk factor for  
918 mood disorders, were related to the degree of aversive pruning across participants.  
919 Taken together, our results suggest a novel circuit in which emotionally salient  
920 information is used to facilitate decision-making, albeit only approximating  
921 optimality. Activation of this circuit could prevent optimal decision-making during  
922 planning and may contribute to psychopathological conditions characterized by  
923 aberrant decision-making.

## Neural Basis of Aversive Pruning

924 **Acknowledgements**

925 We thank Nathaniel Daw for discussions and comments on an earlier draft of the  
926 manuscript.

927

928 **Funding**

929 This work was funded by a British Academy grant (BR10030) to JPR. NL was funded by a  
930 Wellcome Trust-National Institutes of Health joint PhD studentship (WT095465). PF was  
931 funded by an MRC studentship. PD is funded by the Gatsby Charitable Foundation. The  
932 funders had no role in the study design, data collection and interpretation, or the decision to  
933 submit the work for publication.

934

935 **Author Contributions**

936 Conceptualization, J.P.R., N.L., N.E., P.D., and Q.J.M.H.; Design, J.P.R., N.L., N.E., P.D., and  
937 Q.J.M.H.; Data collection, N.L., and P.F.; Writing – Original Draft, J.P.R., N.L., N.E., P.D., P.F.,  
938 and Q.J.M.H.; Writing – Review & Editing J.P.R., N.L., N.E., P.D., P.F., and Q.J.M.H.; Funding  
939 Acquisition, J.P.R. and P.D.; Resources, J.P.R.; Supervision, J.P.R.

940

941 **Competing Interests**

942 The authors declare that no competing interests exist.

943 **References**

944

- 945 **Aldao, A., Nolen-Hoeksema, S. & Schweizer, S.** (2010). Emotion-regulation  
946 strategies across psychopathology: A meta-analytic review. *Clin Psychol Rev* **30**, 217-  
947 37.
- 948 **Amemori, K. & Graybiel, A. M.** (2012). Localized microstimulation of primate  
949 pregenual cingulate cortex induces negative decision-making. *Nat Neurosci* **15**, 776-  
950 85.
- 951 **Beck, A. T., Ward, C. H., Mendelson, M., Mock, J. & Erbaugh, J.** (1961). An inventory  
952 for measuring depression. *Arch Gen Psychiatry* **4**, 561-71.
- 953 **Cooney, R. E., Joormann, J., Eugene, F., Dennis, E. L. & Gotlib, I. H.** (2010). Neural  
954 correlates of rumination in depression. *Cogn Affect Behav Neurosci* **10**, 470-8.
- 955 **Costa, P. & McCrae, R. R.** (1992). The NEO PI-R professional manual. Psychological  
956 Assessment Resources: Odessa, Florida, USA.
- 957 **Dayan, P. & Berridge, K. C.** (2014). Model-based and model-free Pavlovian reward  
958 learning: revaluation, revision, and revelation. *Cogn Affect Behav Neurosci* **14**, 473-  
959 92.
- 960 **Dayan, P. & Huys, Q. J.** (2008). Serotonin, inhibition, and negative mood. *PLoS*  
961 *Comput Biol* **4**, e4.
- 962 **Drevets, W. C., Price, J. L., Simpson, J. R., Jr., Todd, R. D., Reich, T., Vannier, M. &**  
963 **Raichle, M. E.** (1997). Subgenual prefrontal cortex abnormalities in mood disorders.  
964 *Nature* **386**, 824-7.
- 965 **Drevets, W. C., Savitz, J. & Trimble, M.** (2008). The subgenual anterior cingulate  
966 cortex in mood disorders. *CNS Spectr* **13**, 663-81.
- 967 **Eshel, N. & Roiser, J. P.** (2010). Reward and punishment processing in depression.  
968 *Biol Psychiatry* **68**, 118-24.
- 969 **Fales, C. L., Barch, D. M., Rundle, M. M., Mintun, M. A., Snyder, A. Z., Cohen, J. D.,**  
970 **Mathews, J. & Sheline, Y. I.** (2008). Altered emotional interference processing in  
971 affective and cognitive-control brain circuitry in major depression. *Biol Psychiatry* **63**,  
972 377-384.
- 973 **Garrison, J., Erdeniz, B. & Done, J.** (2013). Prediction error in reinforcement  
974 learning: a meta-analysis of neuroimaging studies. *Neurosci Biobehav Rev* **37**, 1297-  
975 310.
- 976 **Geurts, D. E., Huys, Q. J., den Ouden, H. E. & Cools, R.** (2013). Aversive Pavlovian  
977 control of instrumental behavior in humans. *J Cogn Neurosci* **25**, 1428-41.
- 978 **Gotlib, I. H. & Joormann, J.** (2010). Cognition and depression: current status and  
979 future directions. *Annu Rev Clin Psychol* **6**, 285-312.
- 980 **Guitart-Masip, M., Huys, Q. J., Fuentemilla, L., Dayan, P., Duzel, E. & Dolan, R. J.**  
981 (2012). Go and no-go learning in reward and punishment: interactions between  
982 affect and effect. *Neuroimage* **62**, 154-66.

## Neural Basis of Aversive Pruning

- 983 **Huys, Q. J., Daw, N. D. & Dayan, P.** (2015a). Depression: A Decision-Theoretic  
984 Analysis. *Annu Rev Neurosci*.
- 985 **Huys, Q. J., Eshel, N., O'Nions, E., Sheridan, L., Dayan, P. & Roiser, J. P.** (2012).  
986 Bonsai trees in your head: how the pavlovian system sculpts goal-directed choices by  
987 pruning decision trees. *PLoS Comput Biol* **8**, e1002410.
- 988 **Huys, Q. J., Lally, N., Faulkner, P., Eshel, N., Seifritz, E., Gershman, S. J., Dayan, P. &  
989 Roiser, J. P.** (2015b). Interplay of approximate planning strategies. *Proc Natl Acad Sci  
990 U S A* **112**, 3098-103.
- 991 **Johansen-Berg, H., Gutman, D. A., Behrens, T. E., Matthews, P. M., Rushworth, M.  
992 F., Katz, E., Lozano, A. M. & Mayberg, H. S.** (2008). Anatomical connectivity of the  
993 subgenual cingulate region targeted with deep brain stimulation for treatment-  
994 resistant depression. *Cereb Cortex* **18**, 1374-83.
- 995 **Joormann, J. & Gotlib, I. H.** (2010). Emotion regulation in depression: relation to  
996 cognitive inhibition. *Cogn Emot* **24**, 281-98.
- 997 **Jylha, P. & Isometsa, E.** (2006). The relationship of neuroticism and extraversion to  
998 symptoms of anxiety and depression in the general population. *Depress Anxiety* **23**,  
999 281-9.
- 1000 **Krishnan, V. & Nestler, E. J.** (2008). The molecular neurobiology of depression.  
1001 *Nature* **455**, 894-902.
- 1002 **Lamers, F., van Oppen, P., Comijs, H. C., Smit, J. H., Spinhoven, P., van Balkom, A. J.  
1003 L. M., Nolen, W. A., Zitman, F. G., Beekman, A. T. F. & Penninx, B. W. J. H.** (2011).  
1004 Comorbidity patterns of anxiety and depressive disorders in a large cohort study: the  
1005 Netherlands Study of Depression and Anxiety (NESDA). *J Clin Psychiatry* **72**, 341-348.
- 1006 **Mai, J. K., Assheuer, J. & Paxinos, G.** (2003). *Atlas of the human brain*. Elsevier  
1007 Academic Press: San Diego, USA.
- 1008 **Medford, N. & Critchley, H. D.** (2010). Conjoint activity of anterior insular and  
1009 anterior cingulate cortex: awareness and response. *Brain Struct Funct* **214**, 535-49.
- 1010 **Mobbs, D., Petrovic, P., Marchant, J. L., Hassabis, D., Weiskopf, N., Seymour, B.,  
1011 Dolan, R. J. & Frith, C. D.** (2007). When fear is near: threat imminence elicits  
1012 prefrontal-periaqueductal gray shifts in humans. *Science* **317**, 1079-83.
- 1013 **Mobbs, D., Yu, R., Rowe, J. B., Eich, H., FeldmanHall, O. & Dalgleish, T.** (2010).  
1014 Neural activity associated with monitoring the oscillating threat value of a tarantula.  
1015 *Proc Natl Acad Sci U S A* **107**, 20582-6.
- 1016 **Newman, S. D., Carpenter, P. A., Varma, S. & Just, M. A.** (2003). Frontal and parietal  
1017 participation in problem solving in the Tower of London: fMRI and computational  
1018 modeling of planning and high-level perception. *Neuropsychologia* **41**, 1668-82.
- 1019 **O'Doherty, J. P., Hampton, A. & Kim, H.** (2007). Model-based fMRI and its  
1020 application to reward learning and decision making. *Ann N Y Acad Sci* **1104**, 35-53.
- 1021 **Ongur, D., Ferry, A. T. & Price, J. L.** (2003). Architectonic subdivision of the human  
1022 orbital and medial prefrontal cortex. *J Comp Neurol* **460**, 425-49.



## Neural Basis of Aversive Pruning

- 1023 **Palmeri, S., Justo, D., Jauffret, C., Pavlicek, B., Dauta, A., Delmaire, C., Czernecki,**  
1024 **V., Karachi, C., Capelle, L., Durr, A. & Pessiglione, M.** (2012). Critical roles for  
1025 anterior insula and dorsal striatum in punishment-based avoidance learning. *Neuron*  
1026 **76**, 998-1009.
- 1027 **Roiser, J. P., Elliott, R. & Sahakian, B. J.** (2012). Cognitive mechanisms of treatment  
1028 in depression. *Neuropsychopharmacology* **37**, 117-36.
- 1029 **Russell, S. J. & Wefald, E. H.** (1991). *Do the Right Thing: Studies in limited rationality.*  
1030 MIT Press: Cambridge, Massachusetts.
- 1031 **Schultz, W.** (2015). Neuronal Reward and Decision Signals: From Theories to Data.  
1032 *Physiol Rev* **95**, 853-951.
- 1033 **Sheehan, D. V., Lecrubier, Y., Sheehan, K. H., Amorim, P., Janavs, J., Weiller, E.,**  
1034 **Hergueta, T., Baker, R. & Dunbar, G. C.** (1998). The Mini-International  
1035 Neuropsychiatric Interview (M.I.N.I.): the development and validation of a structured  
1036 diagnostic psychiatric interview for DSM-IV and ICD-10. *J Clin Psychiatry* **59 Suppl 20**,  
1037 22-33;quiz 34-57.
- 1038 **Solway, A. & Botvinick, M. M.** (2012). Goal-directed decision making as probabilistic  
1039 inference: a computational framework and potential neural correlates. *Psychol Rev*  
1040 **119**, 120-54.
- 1041 **Spielberger, C. D., Gorsuch, R. L. & Lushene, R. E.** (1970). Test manual for the State-  
1042 Trait Anxiety Inventory. Consulting Psychologists Press: Palo Alto, California.
- 1043 **Talmi, D., Dayan, P., Kiebel, S. J., Frith, C. D. & Dolan, R. J.** (2009). How humans  
1044 integrate the prospects of pain and reward during choice. *J Neurosci* **29**, 14617-26.
- 1045 **Tolman, E. C.** (1948). Cognitive maps in rats and men. *Psychol Rev* **55**, 189-208.
- 1046 **Tversky, A. & Kahneman, D.** (1991). Loss Aversion in Riskless Choice - a Reference-  
1047 Dependent Model. *Quarterly Journal of Economics* **106**, 1039-1061.
- 1048 **Wechsler, D.** (2001). Wechsler Test of Adult Reading Manual. The Psychological  
1049 Corporation: San Antonio, USA.
- 1050 **Weiskopf, N., Hutton, C., Josephs, O. & Deichmann, R.** (2006). Optimal EPI  
1051 parameters for reduction of susceptibility-induced BOLD sensitivity losses: a whole-  
1052 brain analysis at 3 T and 1.5 T. *Neuroimage* **33**, 493-504.
- 1053 **Yu, R., Mobbs, D., Seymour, B. & Calder, A. J.** (2010). Insula and striatum mediate  
1054 the default bias. *J Neurosci* **30**, 14702-7.
- 1055



## Neural Basis of Aversive Pruning

1056 **Figure 1.** Aversive pruning example and fMRI task design. **(A)** Decision tree and  
1057 monetary outcomes up to a depth of three, from starting state 2. Purple and  
1058 orange coloured lines indicate pressing the left and right buttons, respectively.  
1059 The totals earned for the two best paths (thicker lines; breaking even and losing  
1060 20 pence) are shown in blue and red. **(B)** An example of disadvantageous  
1061 aversive pruning. The red line shows the curtailment of search within the  
1062 decision tree upon encountering a large monetary loss (-70p), such that the  
1063 more advantageous break-even sequence is not considered. **(C)** Button presses  
1064 and transitions within the maze. **(D)** Monetary outcomes within the maze. **(E)**  
1065 Free plan trial. Beginning in a selected white box, participants had 9 seconds to  
1066 plan a sequence of moves (3-5; indicated centrally) to maximise income. Plus  
1067 and minus signs below each box indicate the potential outcomes possible from  
1068 moving from there, but are not indicative of directionality. Coloured sidebar  
1069 arrows were included to match visual input with restricted plan trials. **(F)**  
1070 Restricted plan trial. Participants had 9 seconds to decide between two maze  
1071 routes (green and blue), one of which provided higher net income. **(G)** For  
1072 restricted plan trials, the selection of either the blue or green route involved  
1073 choosing either the left or right button. **(H)** After entering their moves or path  
1074 selection, participants were shown their selected path with the corresponding  
1075 monetary outcome for each box-to-box transition for both free and restricted  
1076 plan trials. Summed path totals were not shown.

1077 **Figure 2.** Initial model-free and model-based computational model comparison and  
1078 parameter estimates for behaviour analysis. **(A)** Percentage of trials on which the  
1079 correct sequence was chosen, split by whether it did not include a large loss (green:  
1080 optimal no large loss; ONLL) or did (blue: optimal large loss; OLL). Black dots  
1081 represent individual performance and grey lines connect the two trial types. **(B)**  
1082 ONLL and OLL performance split by decision depth. **(C)** Average likelihood of  
1083 participants' choices. Chance model performance level is shown by the black dashed  
1084 line; "Lookahead" represents optimal planning; "Discount" incorporates random  
1085 stopping of the tree search; "Pruning" additionally incorporates a specific chance of  
1086 stopping when a large loss (-70p) is encountered; and "Pruning+Loss" additionally  
1087 incorporates individual reinforcement value sensitivities to account for loss aversion.  
1088 **(D)** Proportion of variance explained by the different models. **(E)** Model evidence  
1089 measured by group-level iBIC; red star indicates the best performing (i.e. lower iBIC)  
1090 model. **(F)** Pruning parameters (values indicate the probability of continuing to  
1091 evaluate the decision tree). Black dots in F show individual data (parameters taken  
1092 from the Pruning+Loss model), connected by black dashed lines. **(G)** Reinforcement  
1093 sensitivity parameter estimates. **(H)** Relationship between the trial-based measure  
1094 of general planning ability, optimal no large loss (ONLL), and its computational  
1095 equivalent,  $\gamma_G$ . **(I)** Relationship between the trial-based measure of aversive pruning  
1096 (ONLL minus optimal large loss (OLL)) and its computational equivalent, the  
1097 difference between  $\gamma_G$  and  $\gamma_S$ . **(J)** Comparison of ONLL and OLL correct between the  
1098 observed data and data generated from our winning model. **(K)** Observed and  
1099 generated data for each individual subject plotted for ONLL and OLL correct trials.  
1100 **(L)** The fraction of times the winning model gave the highest probability to the  
1101 action chosen by the subject; red line shows chance level. Red and green error bars  
1102 indicate one standard error and 95% confidence intervals of the mean, respectively.

## Neural Basis of Aversive Pruning

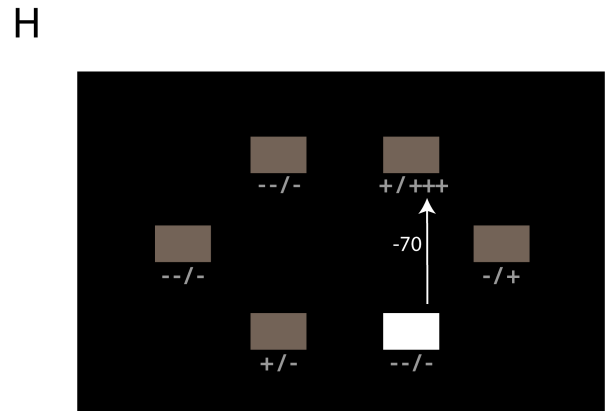
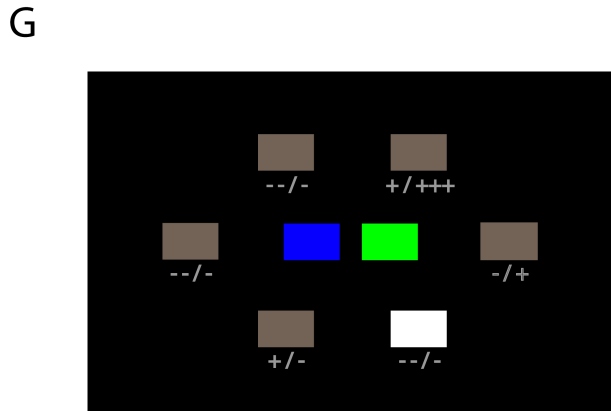
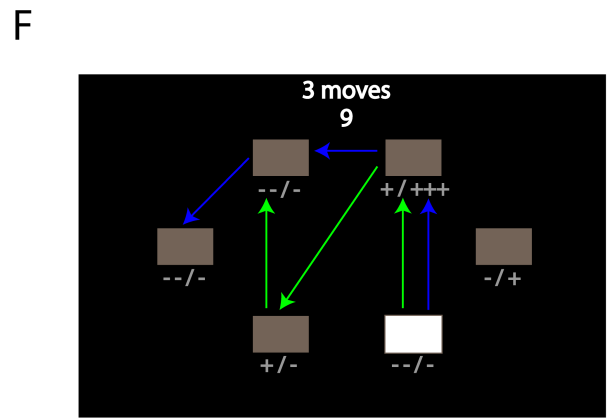
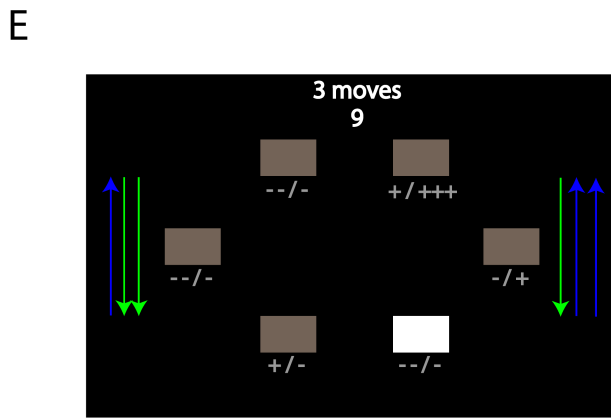
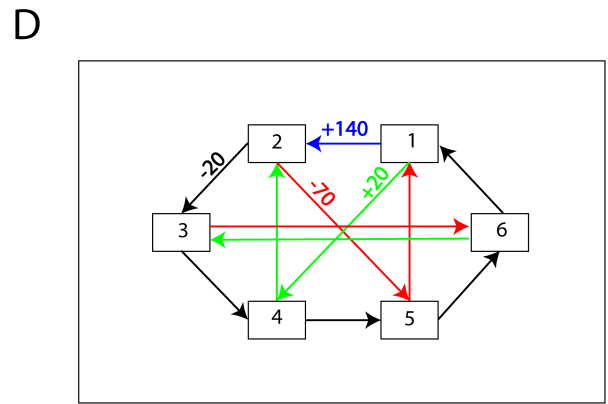
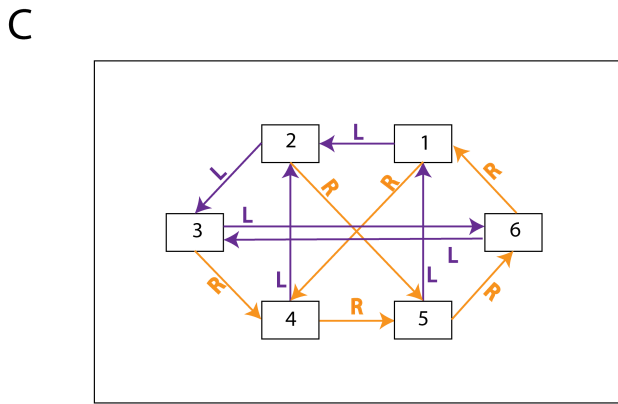
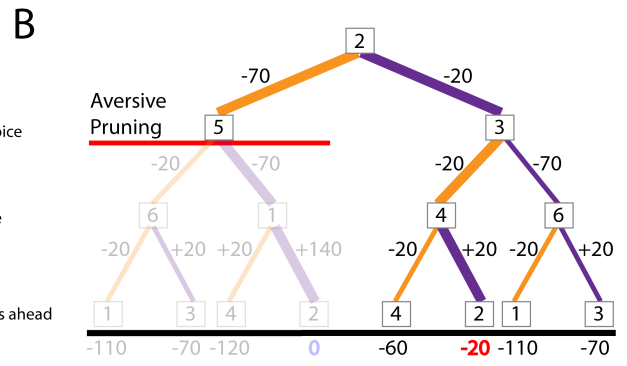
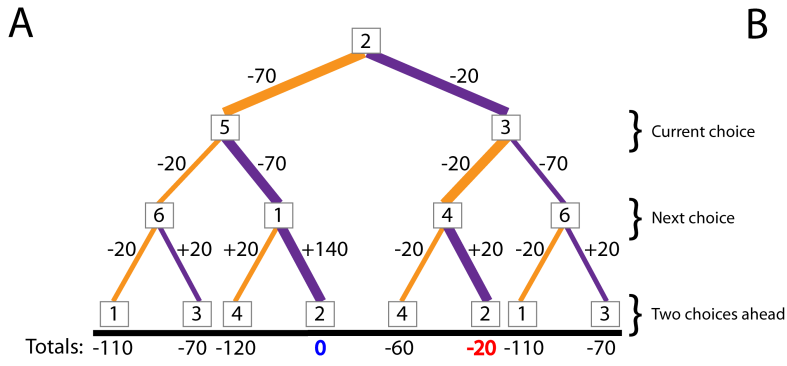
1103 **Figure 3.** Neural responses during aversive pruning: model-based fMRI results.  
1104 **(A)** Kullback-Leibler (KL) divergence value increased linearly with depth, and, **(B)**  
1105 based on participant behaviour, was highest on trials classified as aversive  
1106 pruning trials. **(C)** Activation in pregenual and subgenual cingulate (SGC) cortex  
1107 increased linearly with KL divergence value. **(D)** There was an interaction  
1108 between KL divergence value and difficulty in the SGC, with greater impact of  
1109 the former on more difficult trials. Overlays are presented at a threshold of  $P <$   
1110 0.005 (uncorrected). Error bars represent one standard error of the mean and  
1111 colour bars indicate  $t$ -values.

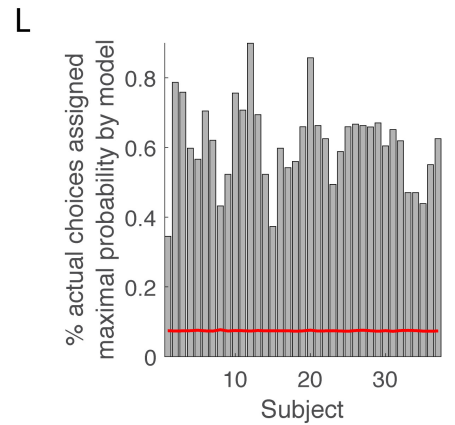
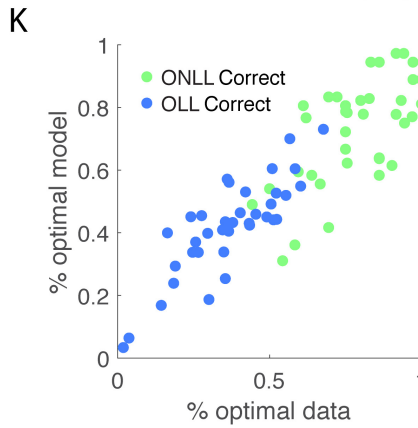
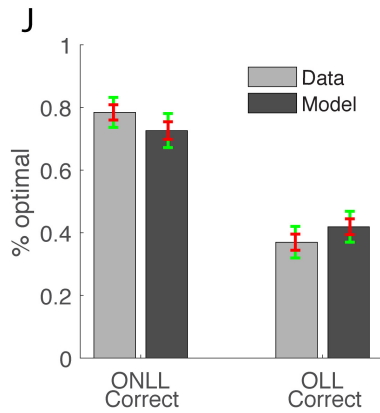
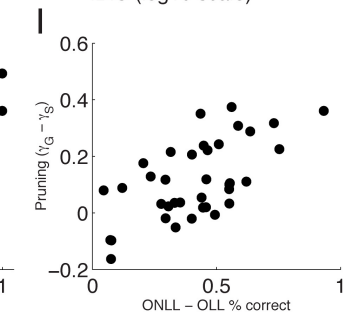
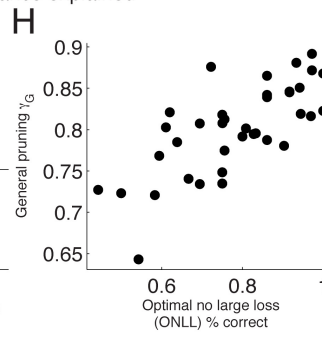
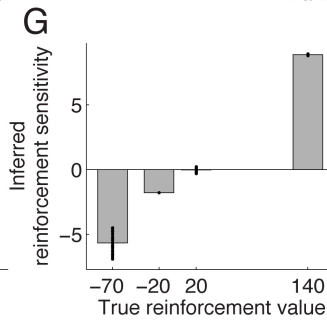
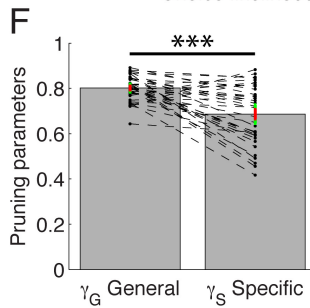
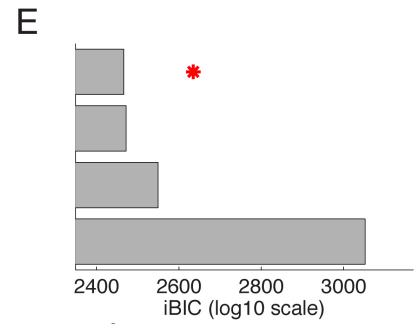
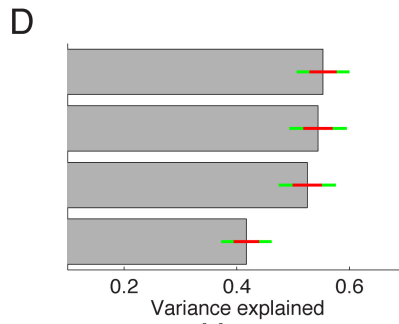
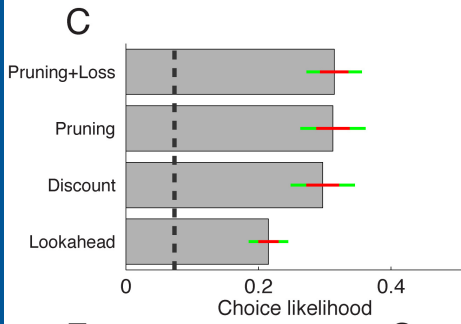
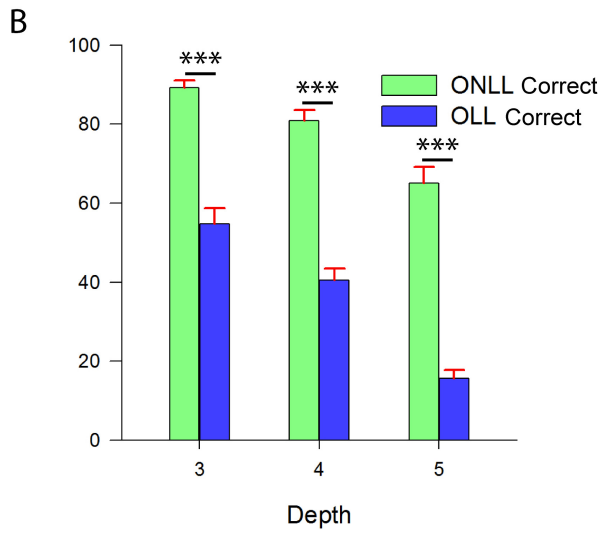
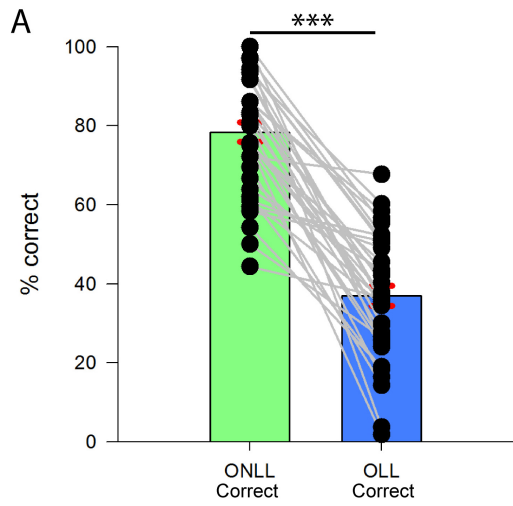
## Neural Basis of Aversive Pruning

1112 **Figure 4.** Neural responses to increasing difficulty and value and relationship between  
1113 aversive pruning and loss receipt at outcome. **(A)** Bilaterally, cerebellum (left panel), motor  
1114 cortex (left panel), dorsal striatum (middle panel), and dorsolateral prefrontal cortex (right  
1115 panel) activation increased linearly with task difficulty during the planning phase. Overlays  
1116 are presented at a threshold of  $P_{WB} < 0.05$ . **(B)** Ventral striatum (VS; left panel) and medial  
1117 orbitofrontal cortex (mOFC, middle panel) activation increased linearly with the net  
1118 monetary value during the outcome phase. Overlays are presented at a threshold of  $P <$   
1119  $0.005$  (uncorrected) but VS and mOFC results survive voxel-level  $P_{WB} < 0.05$ . Peak voxel  
1120 mOFC activation to increasing reward (B, right panel) correlated with the sensitivity to large  
1121 rewards (+140p) parameter derived from our computational model. **(C)** Contrasting  
1122 feedback on the correct trial types (OLL vs ONLL correct) revealed responses in the right  
1123 insula (C, left panel), and right dorsolateral prefrontal cortex (DLPFC; C, left panel). Response  
1124 in the insula was driven by increased activation during OLL correct outcomes (C, middle  
1125 panel). The difference in insula activation between OLL and ONLL correct trials at outcome  
1126 correlated with  $\gamma_G - \gamma_S$ , our computationally-derived measure of overall aversive pruning (C,  
1127 right panel). Overlays are presented at a threshold of  $P < 0.005$  (uncorrected). Error bars  
1128 represent one standard error of the mean and colour bars indicate  $t$ -values.

## Neural Basis of Aversive Pruning

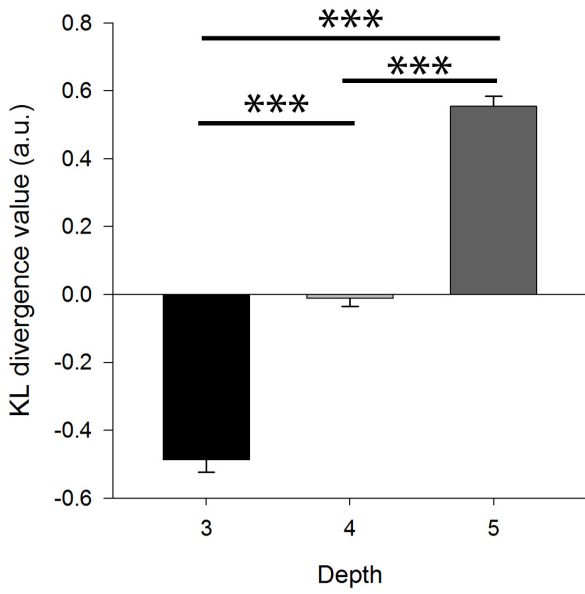
1129 **Figure 5.** Confirmatory trial-based behavioural and fMRI results. **(A)** Decision  
1130 tree showing path selection starting from state 2 with 3 moves to go; line width  
1131 is proportional to selection frequency. The optimal route (break-even, blue) and  
1132 the sub-optimal aversive pruning route (net income -20p, red) were selected  
1133 with similar frequency. **(B)** Aversive pruning percentage [aversive pruning/  
1134 (aversive pruning+OLL error)\*100], split by depth. **(C)** Mean trial  
1135 earnings across the four conditions. The light red bar behind aversive pruning  
1136 depicts the possible earnings if participants had performed optimally on the  
1137 trials classified as aversive pruning. OLL error represents incorrect choices on  
1138 OLL trials that could not be classified as aversive pruning. **(D)** Reaction times for  
1139 the first button press across trial types. **(E)** Difficulty-related response in the  
1140 subgenual cingulate (SGC: left panel) contrasting aversive pruning trials against  
1141 optimal large loss (OLL) correct trials. Overlay is presented at a threshold of  $P <$   
1142 0.005 (uncorrected). The finding in the SGC was driven by a negative  
1143 modulation by difficulty for OLL correct trials ( $P = 0.001$ ), with no significant  
1144 effect of difficulty on aversive pruning trials ( $P = 0.285$ , right panel). Error bars  
1145 represent one standard error of the mean and the colour bar indicates  $t$ -values.



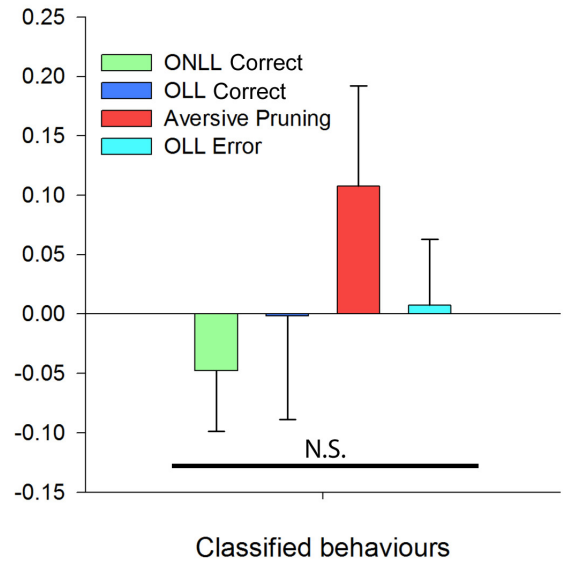




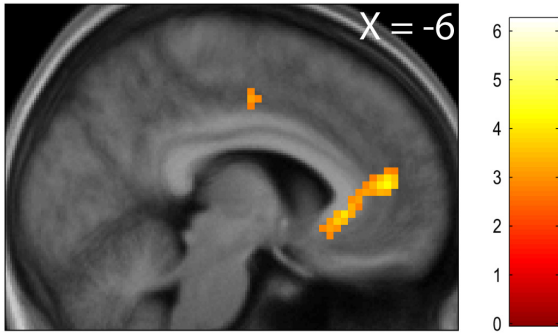
A



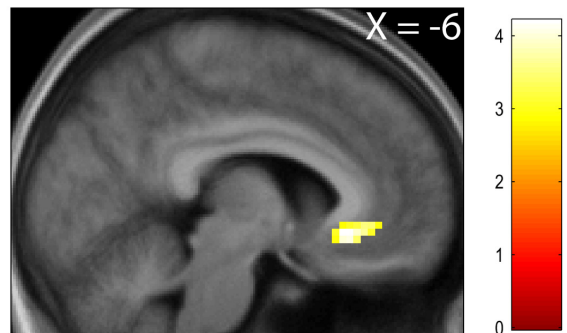
B



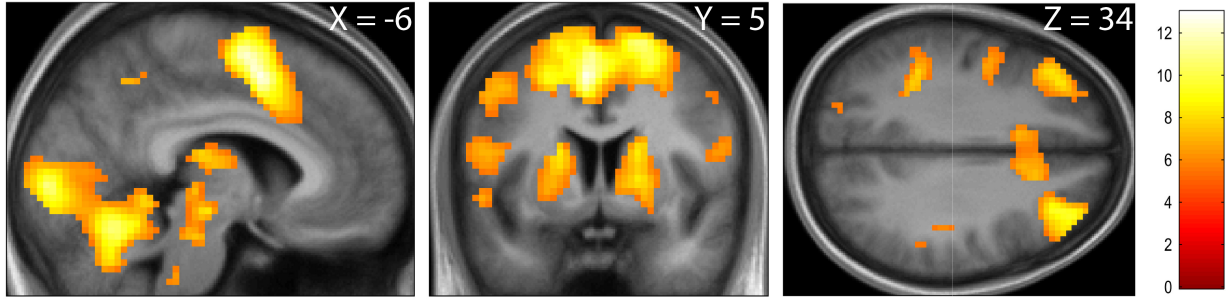
C



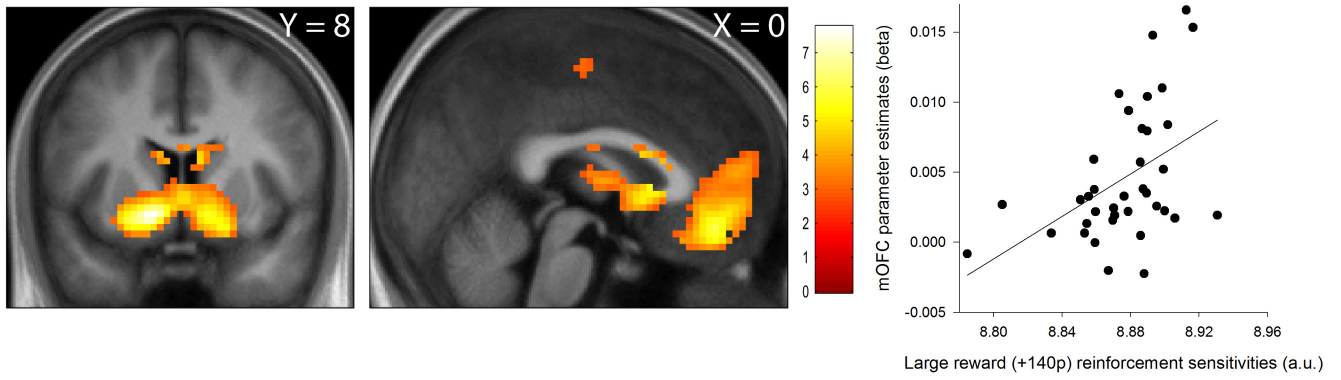
D



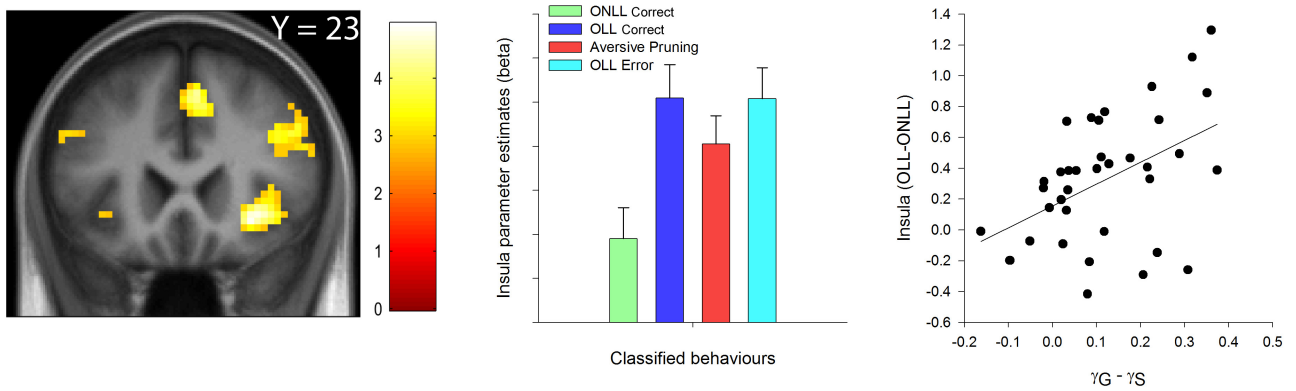
A



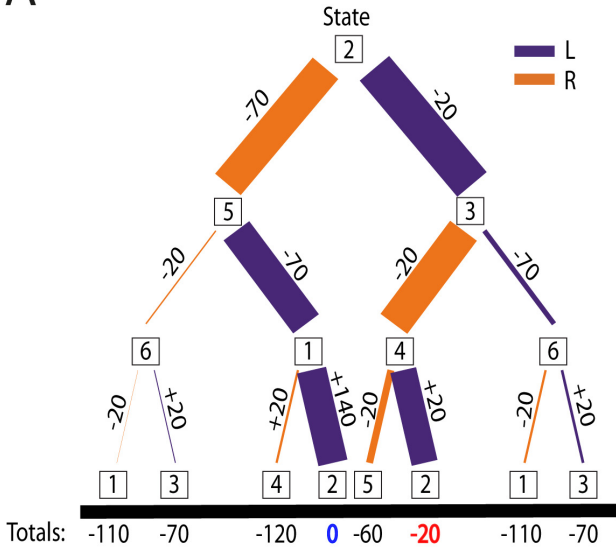
B



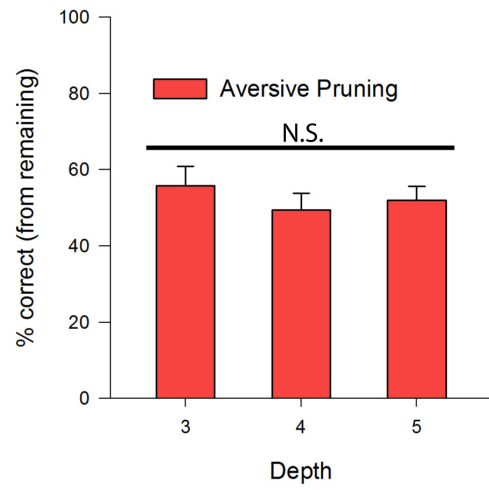
C



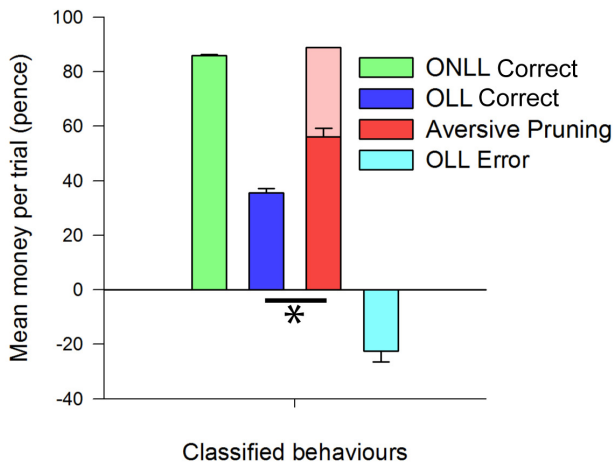
A



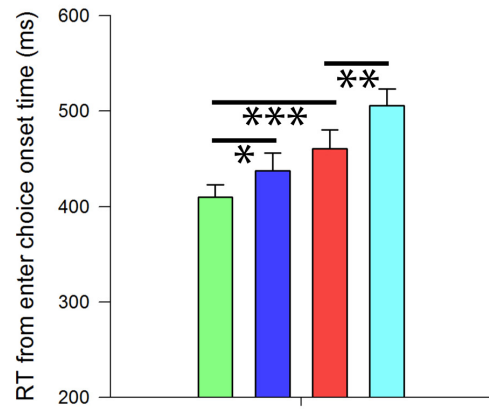
B



C



D



E

